5-1979

Petrology and Mineralogy of Quaternary Basalts, Gem Valley and Adjacent Bear River Range, Southeastern Idaho

William D. Perkins

UtahState University
MERRILL-CAZIER LIBRARY

PETROLOGY AND MINERALOGY OF QUATERNARY BASALTS, GEM VALLEY

AND ADJACENT BEAR RIVER RANGE, SOUTHEASTERN IDAHO

by

William D. Perkins

A thesis submitted in partial fulfillment
of the requirements for the degree

of

MASTER OF SCIENCE

in

Geology

UTAH STATE UNIVERSITY
Logan, Utah

1979

ACKNOWLEDGEMENTS

TABLE OF CONTENTS

LIST OF TABLES

LIST OF FIGURES

ABSTRACT

Petrology and Mineralogy of Quaternary Basalts, Gem Valley

and Adjacent Bear River Range, Southeastern Idaho

by

William D. Perkins, Master of Science

Utah State University, 1979

Major Professor: Dr. Donald W. Fiesinger
Department: Geology

Quaternary basalts of Gem Valley, Idaho, are present as valley fill
(Group 1) and as well defined flows in the Bear River Range (Group 2)
east of Gem Valley. Minerals present in both groups of basalts include
olivine (Fo_{73}-Fo_{39}), augite (Wo_{41} En_{39} Fs_{20}), plagioclase (An_{75}-An_{40}),
and Fe-Ti oxides. Coexisting pairs of magnetite and ilmenite, and
olivine and clinopyroxene in several samples indicate temperatures of
crystallization from 958°C to 1167°C. The Group 2 basalts exhibit a
cumulate texture with abundant large (2 cm) phenocrysts of plagioclase.

Chemically, the Gem Valley basalts are similar to the basalts of
the Snake River Plain with respect to SiO_2, total Fe, P_2O_5 and Na_2O but
differ in the amounts of Al_2O_3 and MgO present. The Al_2O_3 is generally
higher and the MgO is generally lower in the Gem Valley basalts. Com-
paring Group 1 with Group 2 basalts, the Group 2 basalts generally have
more alumina and alkalis than the Group 1 basalts. Chemically both
groups of basalt exhibit characteristics of the tholeiitic basalt suite,

because they are hypersthene normative. Mineralogically, both groups of basalt contain but one pyroxene, augite, which is characteristic of the alkali-olivine basalt suite. This apparent contrast in classifications may be resolved by referring to these basalts as transitional between the alkali-olivine and tholeiitic basalt suites, with the restriction that no genetic relationship to either suite is implied.

Within the limits of this study, it is proposed that the Group 1 basalts may have formed by the partial melting of mantle material with a pyrolite composition. Furthermore, the Group 2 basalts appear to have originated as a result of the accumulation of plagioclase in a fractionating magma of Group 1 composition.

(91 pages)

INTRODUCTION

General Statement

Gem Valley is one of three areas, south of the Snake River Plain, containing Quaternary basalt in southeastern Idaho. Basalt of late Pleistocene age is present as valley fill in Gem Valley and well-defined flows in Nelson and King canyons in the Bear River Range east of Gem Valley.

Previous investigations have shown these basalts to be of similar age and appearance to the basalts of the Snake River Plain (Armstrong et al., 1975; Bright, 1963, 1967). Because of these similarities and the close proximity to the Snake River Plain, the Gem Valley area is ideal for petrologic study and petrogenetic comparison with the basalts of the Snake River Plain.

Purpose of Investigation

The objectives of this investigation are: (1) to determine the chemistry and mineralogy of the basalts of Gem Valley and Nelson and King canyons; (2) to evaluate models of magmatic differentiation and mantle origin; (3) to compare mineralogy, chemistry, and genesis of the basalt present as valley fill in Gem Valley with the basalt present in Nelson and King canyons; and (4) to compare mineralogy, chemistry, and genesis of the basalts of the Gem Valley area with previously published data on the basalts of the Snake River Plain.

Location and Accessibility

The study area (Figure 1) consists of the eastern part of the Ban-
croft quadrangle and the western part of the Soda Springs quadrangle.
The study area covers approximately 100 square miles, and lies wholly
within Caribou County, Idaho.

Gem Valley is situated 36 miles northeast of Preston, Idaho, and
43 miles southeast of Pocatello, Idaho. Soda Springs, Idaho is 5 miles
east of Gem Valley. The town of Grace is situated within Gem Valley.
Portneuf Valley is to the northwest and Gentile Valley is to the south of
Gem Valley.

The study area is accessible from the south along Idaho Route 34
and from the east and west along U.S. 30N.. Roads within Gem Valley,
predominantly light duty dirt and gravel, provide access to within 0.1
mile of areas studied. Access to the Bear River Range, east of Gem
Valley, is by unimproved Forest Service roads. Steepness of these roads
limits access by automobile.

Previous Investigations

Mansfield (1927), in an investigation of the geology of southeastern
Idaho, described lavas in the vicinity of Soda Springs. He classified
the lavas as olivine basalt and described them as having phenocrysts of
olivine, plagioclase, and small amounts of apatite and hematite. Basalt
from the vicinity of Soda Springs may have entered Gem Valley through the
gap at Soda Point (Mabey and Oriel, 1970). In another investigation,
Mansfield (1929) described the lavas in Portneuf Valley, which he also

4
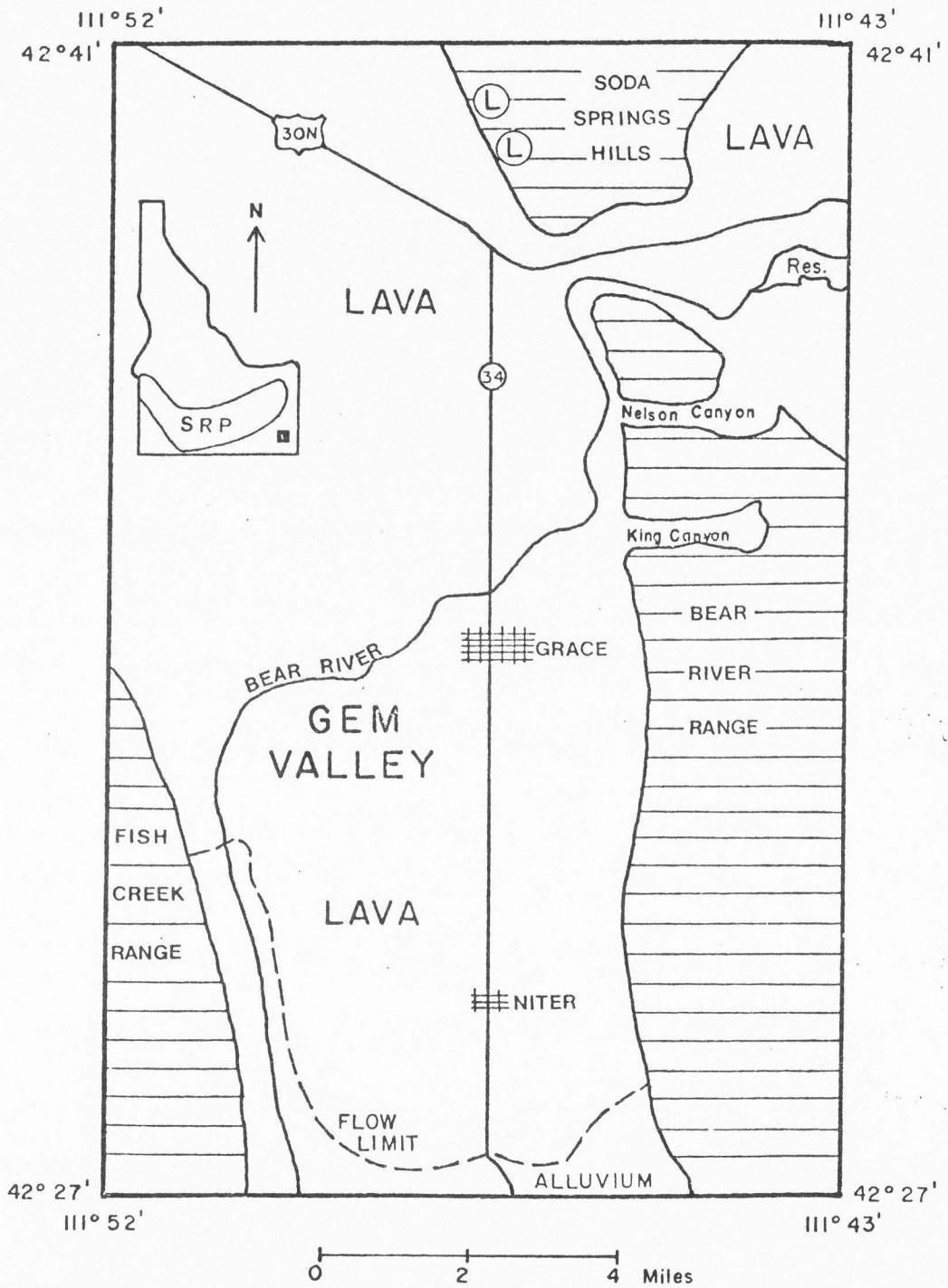
classified as olivine basalt. He described these as having phenocrysts
of plagioclase, olivine, and augite in a groundmass of plagioclase,
olivine, augite, magnetite, and glass.

Bright (1963, 1967) in an investigation of Late Pleistocene stratig-
raphy in the Gem Valley area, named the basalts in Gem Valley the Gem
Volcanics. He classified the Gem Volcanics as porphyritic olivine
basalt. He described the basalt as having phenocrysts of olivine and
plagioclase in a groundmass of plagioclase, olivine, augite, apatite,
and opaques or glass. Bright (1963, 1967) designated the type section
as the west wall of Black Canyon one mile west of Grace. Here he
measured a thickness of 80 feet for the Gem Volcanics, but mentioned
that logs of nearby wells indicated a thickness in excess of 180 feet.

K-Ar dates by Armstrong et al. (1975) indicated an age of 0.1 $\pm$ .03
m.y. for samples of basalt collected in Gem Valley. Bright (1963, 1967)
indicated an age of 33,500 -27,000 years for one flow in Gem Valley based
on stratigraphic relationships with sediments of Lake Thatcher which
were dated by C-14 methods.

A series of geophysical investigations and resulting articles have
dealt with the origin, structure, and pre-basalt topography of Gem
Valley based on gravity and magnetic surveys (Mabey and Armstrong,
1962; Mitchell et al., 1965; Oriel et al., 1965; Mabey and Oriel, 1970;
Mabey 1971). The geologic map of the Soda Springs Quadrangle (Arm-
strong, 1969) and the preliminary geologic map of the Bancroft Quad-
rangle (Oriel, 1968) delineate the extents of the basalt flows and the
locations of eruptive centers.

Geologic Setting

The Gem Valley area lies on the boundary between the northeastern Basin & Range and the western Middle Rocky Mountain physiographic provinces. The boundary between the two provinces is along the western edge of the Bear River Range (Fenneman and Johnson, 1946). The Snake River Plain physiographic province is to the northwest.

Gem Valley is 16 miles long, north-south and has a maximum width of 7 miles. A low divide lies approximately one mile north of the Bear River. The northern part, drained by the Portneuf River, is in the Columbia River drainage system, whereas the southern part, drained by the Bear River, is in the Great Basin drainage system (Mabey and Oriel, 1970).

The Soda Springs Hills (north) and the Bear Range (south) form the eastern boundary of Gem Valley. They are separated by a gap at Soda Point through which the Bear River flows. The Fish Creek Range forms the western boundary of Gem Valley. Rock units in the bordering ranges are predominantly sedimentary rocks of Paleozoic age which may be locally overlain by Tertiary sedimentary units (Mabey and Armstrong, 1962). Stratigraphic investigations of the sedimentary rocks have been made by Mansfield (1927, 1929); Armstrong (1953, 1969); Bright (1963, 1967); Oriel et al. (1965); Oriel (1968); and Mabey and Oriel (1970).

Structural and stratigraphic evidence suggest that Gem Valley is a graben (Mansfield, 1927; Mabey and Armstrong, 1962; Oriel et al., 1965). High-angle normal faults lie along both the western and eastern margins

of Gem Valley (Mabey and Armstrong, 1962). These faults offset both basalt in the valley and Paleozoic rocks in the ranges to the east, evidence for recent activity (Mabey and Armstrong, 1962). Mabey and Oriel (1970) interpreted steep gravity gradients together with a north-south alignment of cinder cones near the eastern margin of Gem Valley as faults along which magma rose to the surface. They also indicated that magnetic anomalies in the vicinity of cinder cones between Grace and Niter may be associated with basalt necks, dikes, and other intrusive units.

Basalt is also present in the Bear River Range, east of Gem Valley. The basalt originated from vents more than 1000 feet above the valley floor, and formed well-defined flows in Nelson and King canyons. Mabey and Oriel (1970) noted the coincidence of these vents with faults in the Bear River Range. They also noted the association of cinder cones along the western edge of the Soda Springs Hills with faults that parallel those in the Bear River Range. No basalt has been found that originated in the Fish Creek Range west of Gem Valley.

Sampling Procedures

Samples were taken from flow units and eruptive centers within Gem Valley and in the Bear River Range and Soda Springs Hills (Figure 2; Table 1). Several samples were taken from each locality. Thin sections were prepared from all samples and used in the selection of samples for more detailed analyses. Those samples which appeared least altered and most representative of the sample area were chosen for further analyses.

To facilitate description and discussion, the samples have been

Figure 2: Sample location map of the Gem Valley area. Filled circles represent locations of samples collected for this study.

Map of Gem Valley showing sample locations.

Label	
111°52'	111°43'
42°41'	42°41'

SODA
SPRINGS
LAVA

(L)

GV77-7 HILLS

30 N

N

LAVA

Res.

GEM
VALLEY

34

GV76-6

GV77-10

GV77-8

GV77-14

BEAR

BEAR RIVER

GRACE

GV77-6

RIVER

RANGE

GV77-13

GV78-1

FISH

GV76-4

CREEK

LAVA

RANGE

NITER

GV78-2

FLOW
LIMIT

ALLUVIUM

42°21'   42°21'
111°52'   111°43'

0   2   4   Miles
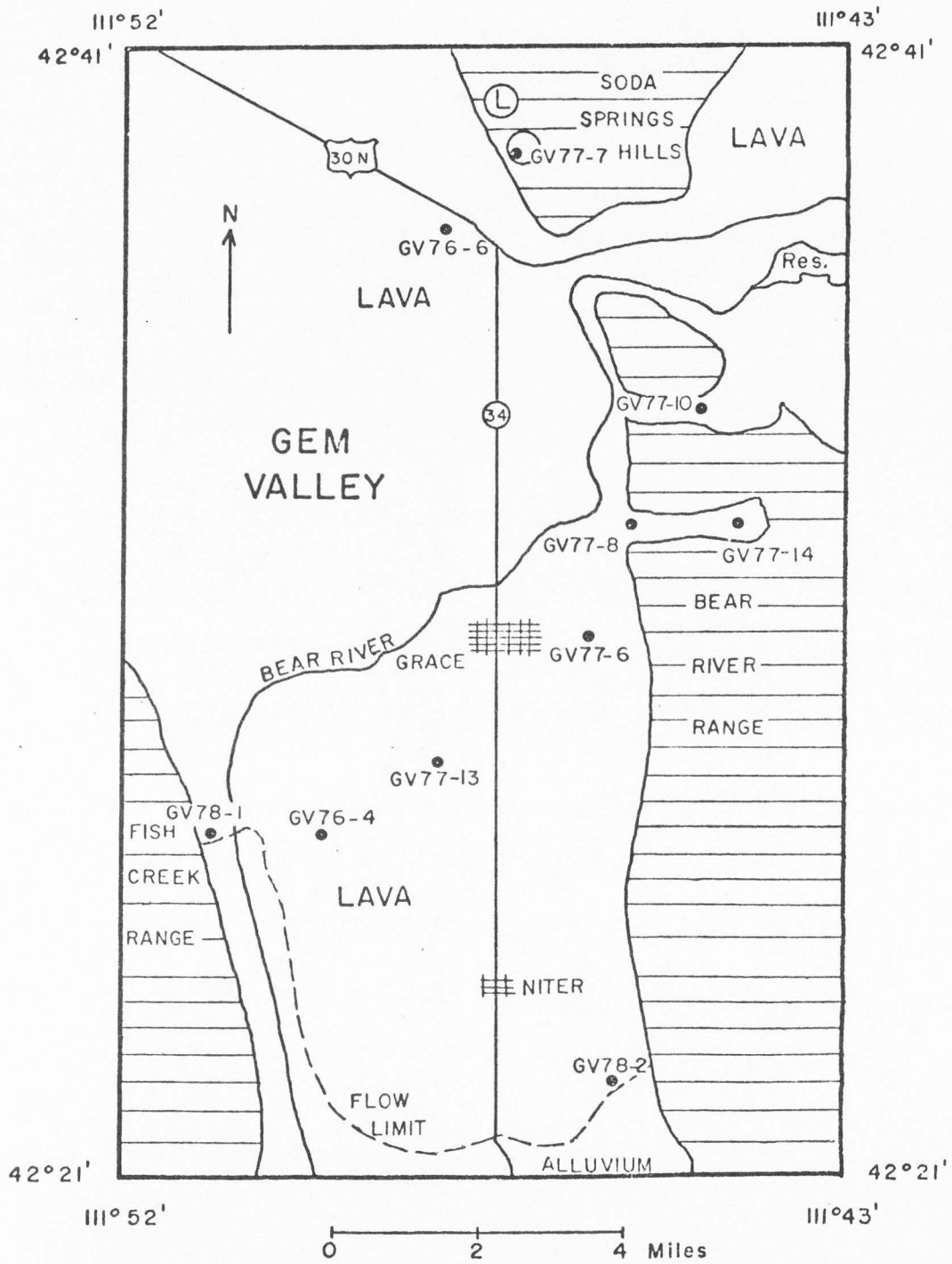
Table 1: Listing of sample codes and locations.

GV76-4   Eruptive center near Cedar Hollow
                (111° 46' W 42° 32' N)

GV76-6   Flow unit from Alexander Crater
                (111° 45' W 42° 39' N)

GV77-6   Fault line east of Grace
                (111° 42' W 42° 35' N)

GV77-7   Southern eruptive center Soda Springs Hills
                (111° 44' W 42° 41' N)

GV77-8   Toe of flow King Canyon
                (111° 42' W 42° 36' N)

GV77-10   Eruptive center Nelson Canyon
                (111° 40' W 42° 37' N)

GV77-13   Active cinder pit southwest of Grace
                (111° 44' W 42° 33' N)

GV77-14   Eruptive center King Canyon
                (111° 40' W 42° 36' N)

GV78-1   Pillow basalt from China Hill road cut
                (111° 50' W 42° 33' N)

GV78-2   Pillow basalt from road cut north of Bittens Ranch
                (111° 42' W 42° 28' N)

---

divided into two distinct groups. Group 1 samples are from flow units
and eruptive centers within Gem Valley. Group 2 samples are from flow
units and eruptive centers in the Bear River Range and Soda Springs
Hills.

PETROGRAPHY

General Statement

The basalts of the Gem Valley area range from dark grey to red in color. All samples observed have vesicles with sizes ranging from less than 0.5 mm up to 2 cm in diameter. The variety of textures observed in these lavas includes ophitic, subophitic, intergranular, cumulophyric, and hyaloophitic. Ophitic to intergranular textures were found in samples from Alexander Crater and in the fault line east of Grace. Hyaloophitic textures are present in the pillow basalts from the road cut near China Hill and the road cut north of Bittens Ranch.

All samples are porphyritic. Phenocrysts of olivine and plagioclase are present in all samples in different amounts. Olivine and plagioclase are also present in the groundmass of all samples. Pyroxene (augite) is visible in the groundmass of most samples. It has been detected by x-ray diffraction techniques in the remaining samples. Magnetite and ilmenite are present in most samples. Results of modal analyses, based on 1000 points counted per slide, are presented in Table 2.

Plagioclase

Plagioclase, the most abundant mineral in all samples, ranges in volume from 25% to 55%. Phenocrysts up to 2 cm long are present in Group 2 basalts, whereas phenocrysts are generally smaller in the Group 1 basalts. Plagioclase phenocrysts are also more abundant in the Group 2

Table 2: Modal analyses of the Gem Valley basalts.

Group & Sample #	Phenocrysts				Groundmass				Undif gdms & Glass	Total
	Olivine	Plagioclase	Pyroxene	Total	Olivine	Plagioclase	Pyroxene	Opaques	Glass	Total
Group 1										
GV76-4	.6	2.5	----	3.1	10.9	25.5	----	30.3	30.2	96.9
GV76-6	2.0	2.2	----	4.2	6.9	37.6	23.7	17.4	10.2	95.8
GV77-6	3.0	3.7	----	6.7	7.4	51.6	23.8	6.0	4.5	93.3
GV77-13	1.8	8.3	----	10.1	8.0	38.2	13.8	16.4	13.5	89.9
GV78-1	5.7	2.7	----	8.4	2.8	24.3	----	----	64.5	91.6
GV78-2	4.3	3.6	----	7.9	3.3	23.0	----	----	65.8	92.1
Group 2										
GV77-7	1.0	3.7	----	4.7	3.9	29.1	2.0	20.1	40.2	95.3
GV77-8	.4	29.3	----	29.7	4.7	19.6	----	19.3	26.7	70.3
GV77-10	1.4	31.1	----	32.5	6.6	15.2	----	21.4	24.3	67.5
GV77-14	2.0	32.4	----	34.4	4.7	7.5	----	14.0	39.4	65.6

basalts (24% by volume) than in the Group 1 basalts (4% by volume).
However, the average total abundance of plagioclase (phenocrysts plus
groundmass) is nearly equal in both (37% in Group 1 basalts, 42% in
Group 2 basalts).

Broken phenocrysts are more common in the Group 2 basalts than in
the Group 1 basalts. Also, many of the phenocrysts in the Group 2
basalts show evidence of resorption and recrystallization. In thin
section GV77-8 one phenocryst has a well-rounded plagioclase core sur-
rounded by a euhedral plagioclase rim. Many of the Group 2 phenocrysts
have an angular appearance probably due to breakage upon eruption.
Very few of the Group 1 lavas show evidence of broken or resorbed plagi-
clase.

Cumulophyric clots of phenocrysts of plagioclase or of plagioclase
and olivine are common in the Group 1 lavas, but rare or absent in the
Group 2 lavas. Groundmass plagioclase is always in the form of small,
subhedral laths. In most samples the laths are randomly oriented.
However those from Alexander Crater have a subparallel to parallel
alignment.

Albite and Carlsbad-Albite twinning is present in plagioclase in
all samples. The Albite twinning dominates. Normal concentric zoning
is present in plagioclase in both Group 1 and Group 2 basalts. The most
striking example of concentric zoning is in sample GV76-6 (Figure 3).
The presence of irregular zoning in the Group 2 lavas may indicate suc-
cessive stages of resorption and recrystallization (Figure 4). Zoning
is not apparent in the groundmass laths in thin section. This absence
may be the result of more rapid crystallization of the groundmass phase.

Figure 3: Plagioclase phenocryst with concentric zoning. Photomicrograph of sample GV76-6. Field of view is 2.0 mm.

Figure 4: Plagioclase phenocryst with irregular zoning. Photomicrograph of sample GV77-8. Field of view is 2.0 mm.
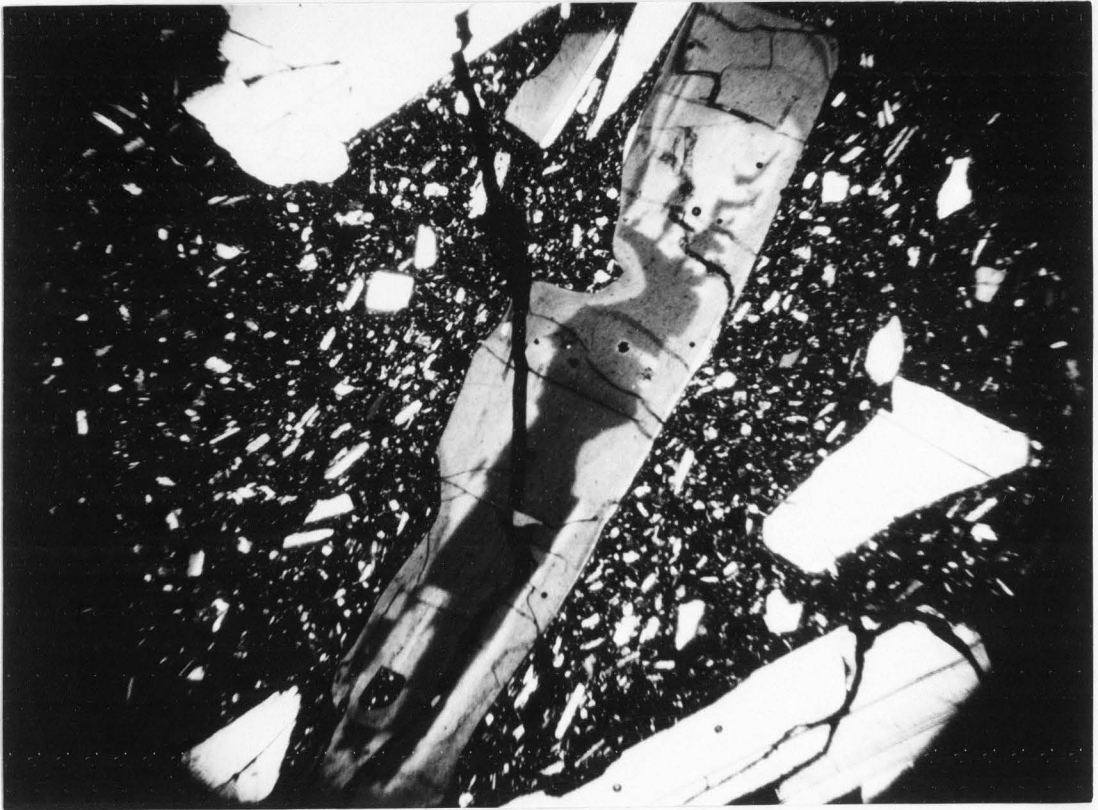
Olivine

Olivine forms phenocrysts up to 3 mm in length. In contrast to plagioclase, the largest phenocrysts of olivine are in the Group 1 lavas. Bright (1963) reported that olivine phenocrysts in the Gem Volcanics range up to 10 mm long and average 2 mm in length. The average size of phenocrysts observed in this study is 1 mm. Alteration is common along the edges and in the cracks of the phenocrysts. This alteration appears red-brown to red-orange in color. In most samples, euhedral crystals of Fe-Ti oxide form inclusions in the phenocrysts. In some samples, generally Group 1 basalts, olivine phenocrysts are almost completely replaced by Fe-Ti oxides (Figure 5). The combination of alteration and apparent subsequent oxidation renders some of the phenocrysts almost completely opaque. The phenocrysts are generally euhedral to subhedral. Groundmass olivine appears less altered, although in some samples, especially those from Niter Cone, the same red-brown alteration is in the groundmass. Groundmass olivine ranges from .01 mm to .5 mm, and is generally present as granules or as intergranular filling. As previously mentioned olivine phenocrysts locally form clots, that may also contain plagioclase phenocrysts, in Group 1 basalts. This cumulophyric texture is also present in the groundmass of some samples. No evidence of zoning of phenocrysts or of groundmass is visible in thin section.

Pyroxene

Pyroxene (augite) is present in both Group 1 and Group 2 basalts. Augite was detected in some samples only by x-ray diffraction. Augite

Figure 5: Phenocryst of olivine with replacement by Fe-Ti oxides.

Photomicrograph of sample GV76-6. Field of view is 2.0 mm.
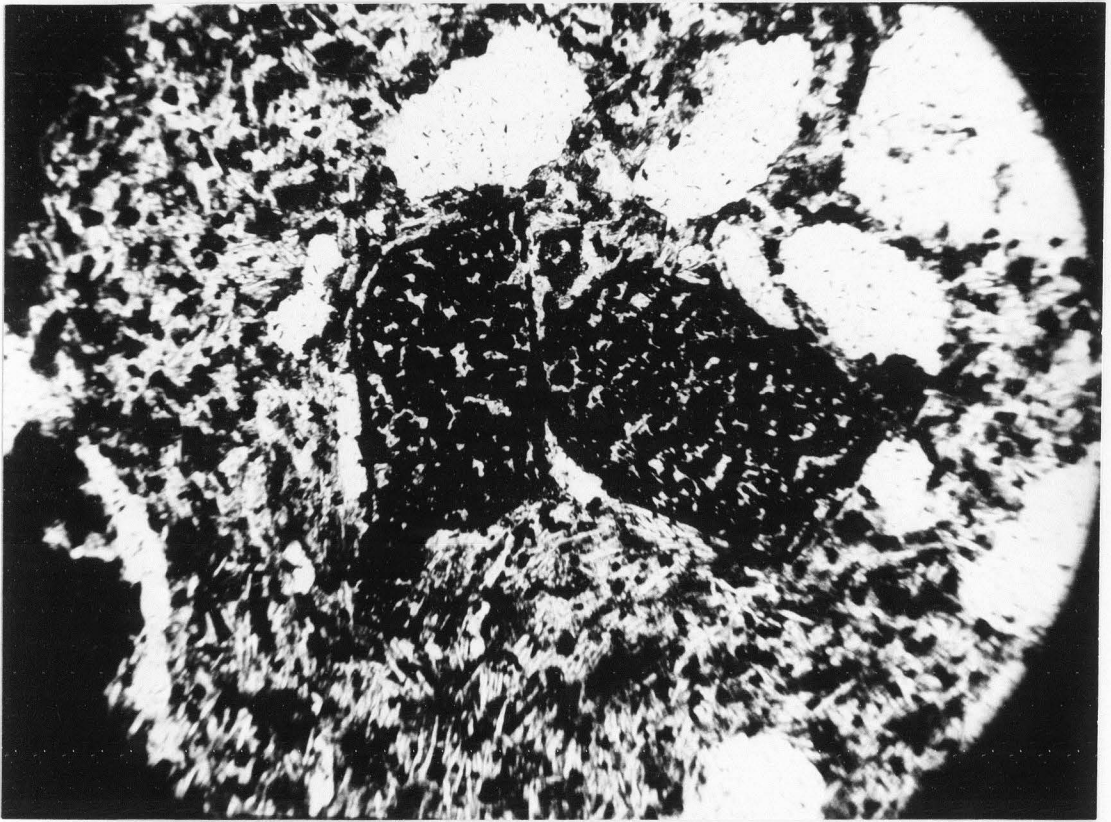
generally forms interstitial fillings between plagioclase laths in a subophitic to ophitic texture. In thin section GV77-7 augite is present as very small but discrete crystals in the groundmass. The augite appears tan and unaltered in thin section. Although it has not been observed as a phenocryst phase, Mansfield (1927, 1929) has reported augite phenocrysts from Portneuf Valley and the Soda Springs area. The maximum amount of augite observed in this study was 24% by volume in the basalt from the fault line east of Grace (GV77-6). Bright (1963) reported up to 45% pyroxene in holocrystalline samples of the Gem Volcanics. In several samples the groundmass was too finely crystalline for accurate mineral identification. If some of the weakly birefringent areas were pyroxene, the total amount of pyroxene observed would increase 3% to 6%.

Fe-Ti Oxides

Magnetite and ilmenite are present in most samples as micropheno-crysts up to .3 mm in diameter and as smaller crystals in the groundmass. In most samples, of which polished sections were made, both the magnetite and ilmenite are exsolved. Two samples (GV76-4, GV76-6) have unaltered magnetite and ilmenite and one sample (GV77-14) has unaltered magnetite and no ilmenite. The exsolved ilmenite generally forms a criss-crossed graphic texture with the lamellae varying in width or compound grains of magnetite and ilmenite. In some samples almost all the magnetite has been exsolved. Magnetite crystals generally form in well-developed cubes. The ilmenite crystals are generally lath shaped to acicular. In pillow basalts opaques are disseminated throughout the groundmass. Identification of discrete crystals can be made only by reflected light. In samples with both magnetite and ilmenite, magnetite appears to be more abundant

than ilmenite. The total abundance of opaques ranges from trace amounts to 30% by volume. In some samples the abundance of opaques estimated may be slightly high due to the disseminated nature of the opaques.

Apatite

Apatite is a ubiquitous phase in the Group 1 basalts. It forms long thin needles barely visible in thin section. Its abundance is less than 1%. No apatite was observed in the Group 2 basalts. However, this may be the result of the extremely fine-grained nature of the groundmass.

Glass

Trace amounts of interstitial glass are present in most samples. It contains abundant microlites and it is usually brown in color. Glass is most abundant in the pillow basalts. The color of the glass in the pillow basalts is tan. The glass is effectively rendered opaque by increased amounts of disseminated Fe-Ti oxides. Bright (1963) identified the tan glass as palagonite. However, Moore (1966) described palagonite rinds on marine pillows in Hawaii as having minute botryoidal bands in sharp contact with the glass. This is not present in the pillows from Gem Valley. Furthermore, Moore (1966) stated that the rate of palagonitization is increased in salt water. The pillows he studied were from 130,000 to 360,000 years old, and the palagonite rinds were from 2 to 10 microns thick. The Hawaiian pillows are older and the palagonite rinds significantly thinner than the rinds Bright (1963) identified. For these reasons the tan rinds probably are glass and not palagonite.

An unusual feature of the pillows, described by Bright (1963), is occurrence of multiple concentric rinds of tan glass (Figure 6). These rinds are most common in the pillows from the east side of the valley (GV78-2). The bands of glass, 2-4 cm thick, are separated by 2-8 cm of opaque groundmass. The contact between the tan glass and the opaque groundmass is gradational through a distance of about 2 mm (Figure 7). In this transitional interval there is an increase of disseminated opaques in the glass until all the glass is rendered opaque. The tan glass encloses crystals of olivine and plagioclase. The abundance of crystals of olivine and plagioclase in the rind is slightly less than in the areas between the rinds. The orientation of the crystals in the rind appears random. This perhaps eliminates flowage differentiation as a mechanism for their formation.

Xenoliths and Xenocrysts

Xenoliths of silt are present in samples from Cedar Hollow (GV76-4). The xenoliths are tan to black in color. Some xenoliths contain small grains of quartz. The area surrounding each xenolith is generally black and opaque, perhaps due to more rapid cooling near the xenolith. The xenoliths are also darker along their edges, which suggests a possible baking effect from the heat of the enclosing melt. Xenocrysts of quartz are also present in samples from Cedar Hollow. The quartz grains are generally well-rounded and surrounded by a fine-grained to opaque groundmass. The lack of a clear, sharp boundary between the quartz and the groundmass indicates that a reaction between the melt and the quartz may have taken place prior to cooling. Bright (1963) suggested that the silt and quartz were derived from sediments of Lake Thatcher.

Figure 6: Pillow basalt with multiple rinds of tan-weathered glass.
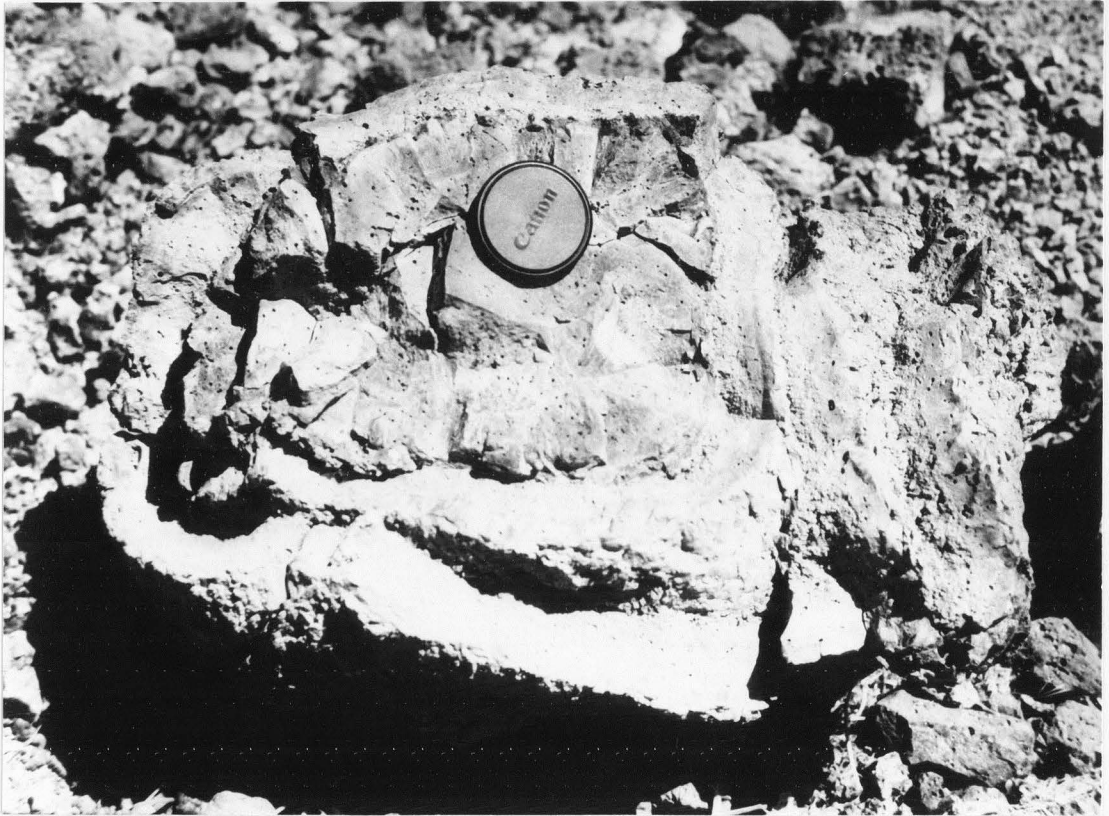
Figure 7: Photomicrograph of pillow basalt, illustrating gradation from transparent glass to glass rendered opaque by disseminated Fe-Ti oxides. Field of view is 7.0 mm.

A xenocryst of orthopyroxene, enstatite, is present in sample GV77-8 (Figure 8). The xenocryst is 3 mm long and is surrounded by a reaction rim .05 mm thick. The rim is composed of finely crystalline olivine and augite, determined by electron-microprobe analysis. Olivine is the predominant phase in the rim. The xenocryst is tan when viewed in plain light, and shows no evidence of alteration other than the reaction rim.

Figure 8: Photomicrograph of pyroxene xenocryst in sample GV77-8. Field of view is 2.0 mm.
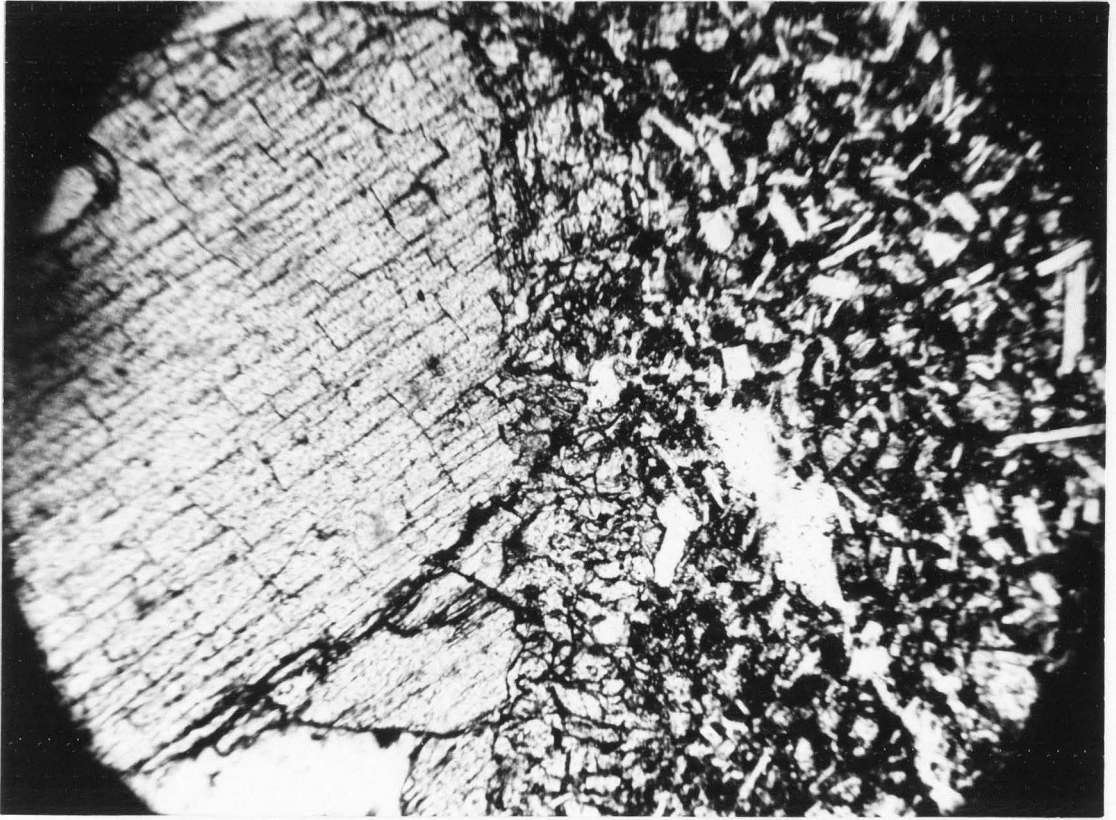
MINERALOGY

Analytical Techniques

Mineral analyses were completed on nine samples: GV76-4, GV76-6, GV77-6, GV77-7, GV77-10, GV77-13, GV77-14, GV78-1, GV78-2. In addition the OPX xenocryst in GV77-8 was also analyzed. The analyses were conducted with an ARL EMX SM electron microprobe at the Department of Geology & Geophysics, University of Utah. In most samples 30-60 spots were anaylzed per mineral. Due to the difficulty in finding suitable Fe-Ti oxides for analyses as few as 10 spots were analyzed per mineral for Fe-Ti oxide composition. Bence and Albee (1968) and Albee and Ray (1970) have outlined correction procedures for data obtained from the electron microprobe. These correction procedures have been incorporated into the computer program SLAVE (Nicholls et al., 1977). This program was used in the reduction of data obtained from the electron microprobe. The standards used in each analysis are presented in Appendix I.

Plagioclase

Plagioclase is the only feldspar present in the basalts of the Gem Valley area. The composition ranges from bytownite (An_{75}) to andesine (An_{40}) in the Group 1 basalts, whereas the composition remains in the range of labradorite (An_{70}-An_{50}) for the Group 2 basalts. Average compositions for both the Group 1 (An_{65}) and the Group 2 (An_{60}) basalts are in the labradorite field. Table 3 shows the average compositions of

Table 3: Average partial microprobe analyses of plagioclase. (p)=phenocryst, (G)= groundmass

Group 1

Sample numbers

	GV76-4 P	GV76-4 G	GV76-6 P	GV76-6 G	GV77-6 P	GV77-6 G	GV77-13 P	GV77-13 G
CaO	14.35	13.43	15.05	13.33	12.98	12.65	13.84	12.79
Na_2O	3.22	3.69	2.91	3.77	4.02	4.21	3.58	4.04
K_2O	.22	.32	.23	.41	.34	.36	.28	.42
Weight percent endmembers								
An	71.20	66.58	74.68	66.14	64.43	62.74	68.47	63.45
Ab	27.23	31.27	24.55	31.84	34.00	34.92	30.24	34.18
Or	1.34	1.86	1.31	2.45	1.99	2.13	1.63	2.47
Total	99.77	99.71	100.54	100.43	100.42	99.79	100.34	100.10
Molecular percent endmembers								
An	70.20	65.53	73.19	64.19	62.90	61.13	67.01	62.09
Ab	28.49	32.65	25.51	32.97	35.16	36.79	32.20	35.49
Or	1.31	1.83	1.29	2.40	1.94	2.07	1.59	2.43

Table 3: continued

Group 1   Group 2

Sample numbers

	GV78-1 P	GV78-1 G	GV78-2	GV77-7 P	GV77-7 G	GV77-10 P	GV77-10 G	GV77-14 P	GV77-14 G
CaO	15.08	13.85	14.08	12.01	11.00	12.89	12.39	12.82	12.71
Na_2O	2.76	3.43	3.41	4.39	4.93	4.02	4.26	4.02	4.13
K_2O	.24	.38	.26	.43	.56	.38	.37	.40	.37

Weight percent endmembers

	GV78-1 P	GV78-1 G	GV78-2	GV77-7 P	GV77-7 G	GV77-10 P	GV77-10 G	GV77-14 P	GV77-14 G
An	74.77	68.68	69.86	59.59	54.58	63.93	61.46	63.53	63.01
Ab	23.41	29.04	28.84	37.11	41.72	34.06	36.06	33.99	34.93
Or	1.39	2.23	1.55	2.56	3.33	2.25	2.17	2.35	2.24
Total	99.57	99.95	100.24	99.26	99.63	100.24	99.69	99.87	100.18

Molecular percent endmembers

	GV78-1 P	GV78-1 G	GV78-2	GV77-7 P	GV77-7 G	GV77-10 P	GV77-10 G	GV77-14 P	GV77-14 G
An	74.04	67.53	68.48	58.67	53.35	62.48	60.32	62.33	61.59
Ab	24.59	30.28	30.00	38.78	43.39	35.33	37.55	35.37	36.22
Or	1.38	2.19	1.52	2.51	3.26	2.20	2.13	2.30	2.18

plagioclase in the analyzed samples. Phenocrysts in all samples zone
to and overlap the groundmass composition. Figure 9 illustrates zoning
trends of the plagioclase in the Gem Valley basalts. Both Group 1 and
Group 2 basalts show trends towards increasing Na and K.

Group 2 basalts, which have larger and more abundant phenocrysts,
exhibit the least amount of zoning. This would suggest a slow develop-
ment of the phenocryst phase allowing the phenocrysts to remain in
equilibrium with the melt or a churning in the magma chamber keeping
the developing crystals mixed throughtout the magma. Mixing in the magma
chamber might also explain the presence of broken phenocrysts in the
Group 2 basalts.

The greatest amount of zoning is in sample GV77-6. The zoning in
this sample, which is from the fault scarp east of Grace, reflects an
envionment of slower cooling in the central portion of the lava flow.

Also shown in Figure 9 is a plot of normative feldspar composition.
It is noteworthy that 8 samples lie to the right of the dashed line in
the two feldspar field indicating the potential crystallization of both
plagioclase and alkali feldspar. This is characteristic of the alkali-
olivine basalt suite.

Chemically the plagioclase found in the Gem Valley basalts lies
within the range of plagioclase compositions reported for basalts from
the Snake River Plain (Stout and Nicholls, 1977; Leeman et al., 1976;
Leeman and Vitaliano 1976).

<div align="center">Olivine</div>

Olivine, in Group 1 basalts, is present in a continuous gradation

Figure 9:   Electron-microprobe analyses of plagioclase plotted in terms
of anorthite (An), albite (Ab), and orthoclase (Or).   Solid triangles:
average phenocryst composition; solid squares: average groundmass com-
position.   Also shown are the normative feldspar compositions.

An   An

Group 1   Group 2

GV76-4   GV76-6   GV77-6   GV77-13   GV78-1   GV78-2   GV77-7   GV77-10   GV77-14

Normative Feldspars

Ab   Or
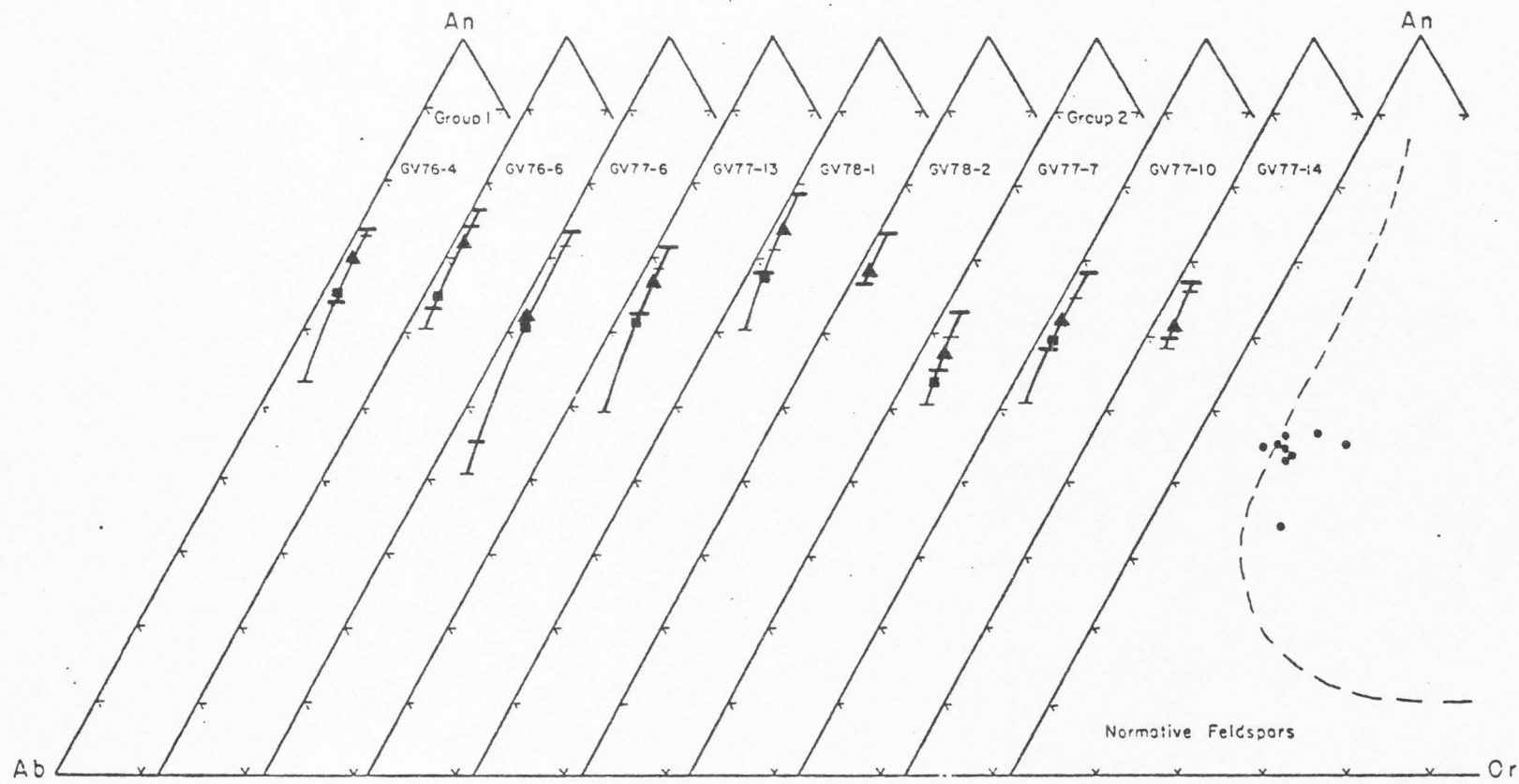
of size from phenocryst to groundmass. This suggests that olivine crystallized throughout most of the crystallization history of these basalts. The average analyses of olivine phenocrysts and groundmass are presented in Table 4. Rims of the olivine phenocrysts zone to and overlap the composition of the groundmass olivine (Figure 10). In Group 2 basalts olivine phenocrysts are rare or absent. Olivine is present primarily as a groundmass phase.

CaO content ranges from .74 wt % to .22 wt %. Simkin and Smith (1970) correlated the CaO content in olivine with the crystallization environment and the bulk chemistry of the host rock. They found that olivines with more than .1 wt % CaO crystallized as shallow intrusives or as extrusives. This suggested that Ca content in olivine is pressure dependent. Stormer (1973) studied CaO content in olivines and its relationship to silica activity and pressure. He found that the initial composition of the olivines depended on the level of silica activity. He also noted that zoning trends may be controlled by the pressure/temperature history of the magma. Rapid increases in Ca content may indicate that a pressure drop was the dominant factor, whereas constant to decreasing Ca content may indicate a cooling trend was the dominant factor.

A plot showing the CaO trend (Figure 11) from phenocryst to groundmass shows that most Group 1 samples have increasing CaO with increasing FeO. This is roughly parallel to the trend of alkali-olivine basalts. An exception to this trend is found in GV76-6 where CaO is decreasing with increasing FeO. This is comparable to the trend exhibited by tholeiitic basalts. The pressure drop may have been slower, whereas decreasing temperature may have been the dominant factor in this sample.

Table 4: Average partial microprobe analyses of olivine. (p)=phenocryst, (G)=groundmass

Group 1

Sample numbers

	GV76-4 P	GV76-4 G	GV76-6 P	GV76-6 G	GV77-6 P	GV77-6 G	GV77-13 P	GV77-13 G
FeO	23.29	27.22	24.65	41.52	27.07	41.56	25.00	36.07
MgO	38.50	35.01	36.50	23.32	34.98	23.05	36.54	27.82
CaO	.39	.51	.43	.38	.39	.49	.38	.50

Weight percent endmembers

	GV76-4 P	GV76-4 G	GV76-6 P	GV76-6 G	GV77-6 P	GV77-6 G	GV77-13 P	GV77-13 G
Fa	33.04	38.61	34.95	58.07	38.40	58.94	35.45	51.16
Fo	67.18	61.08	63.71	40.71	61.06	40.23	63.77	48.55
La	.59	.79	.66	.59	.60	.76	.58	.80
Total	100.81	100.48	99.32	100.71	100.06	99.93	99.80	100.51

Molecular percent endmembers

	GV76-4 P	GV76-4 G	GV76-6 P	GV76-6 G	GV77-6 P	GV77-6 G	GV77-13 P	GV77-13 G
Fa	24.46	30.19	27.83	49.68	30.34	50.03	27.63	41.81
Fo	72.80	69.07	71.54	49.73	69.10	49.21	71.83	57.45
La	.53	.73	.61	.60	.56	.76	.54	.75

Table 4:   Continued

	Group 1				Group 2		
	Sample numbers						
	GV78-1 P	GV78-1 G	GV78-2 P	GV78-2 G	GV77-7 G	GV77-10 G	GV77-14 G
FeO	22.29	27.71	21.42	26.10	26.54	39.07	28.67
MgO	38.61	34.02	39.67	35.10	35.63	25.80	33.61
CaO	.42	.55	.40	.54	.39	.26	.39
	Weight percent endmembers						
Fa	31.62	39.29	30.38	37.02	37.64	55.42	40.65
Fo	67.39	59.38	69.24	62.68	62.19	45.02	58.65
La	.65	.84	.61	.83	.60	.39	.59
Total	99.65	99.51	100.23	100.52	100.43	100.83	99.90
	Molecular percent endmembers						
Fa	24.35	31.16	23.16	28.84	29.30	45.78	32.23
Fo	75.07	68.05	76.29	70.38	69.78	53.84	67.21
La	.59	.79	.55	.79	.56	.39	.56

Figure 10: Electron-microprobe analyses of olivine plotted in terms of forsterite (Fo) and fayalite (Fa). P: phenocryst; G: groundmass; solid triangles: average composition; bars: range for phenocryst and groundmass of each sample.

Group 1

GV76-4

GV76-6

GV77-6

GV77-13

GV78-1

GV78-2

Group 2

GV77-7

GV77-10

GV77-14

Fo   90   80   70   60   50   40   30   20   10   Fa
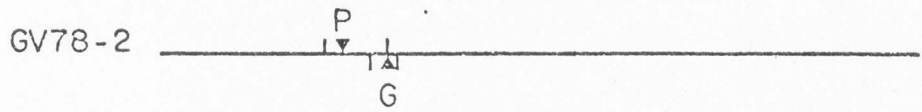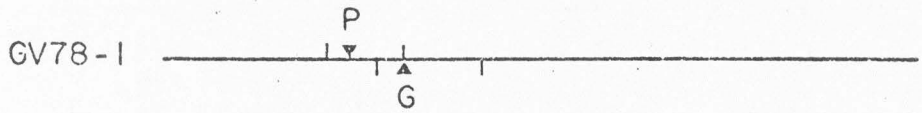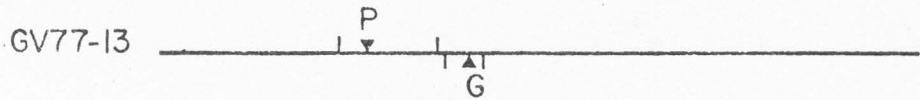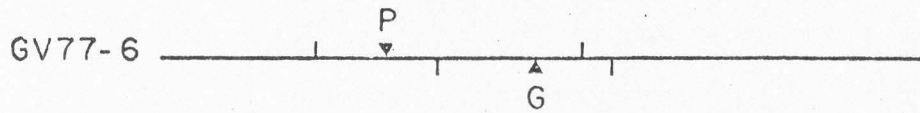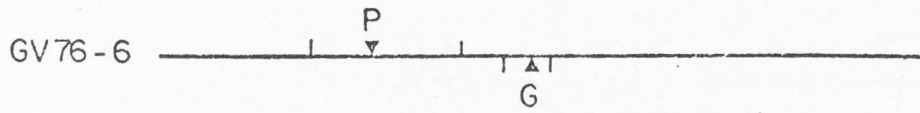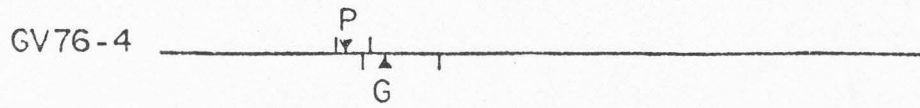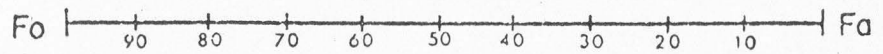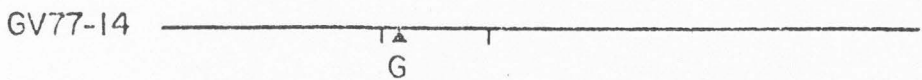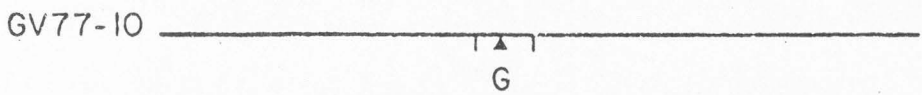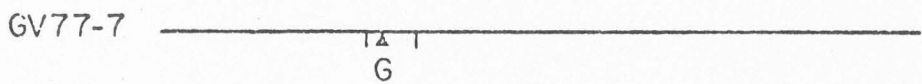
Figure 11: CaO and FeO contents of olivine in the basalts of the Gem

Valley area. Open circles: Group 1 phenocrysts; filled circles: Group

1 groundmass; filled squares: Group 2 groundmass. Lines connect coex-

isting phenocryst and groundmass phases. Olivine from tholeiitic basalt

(Moore and Evans, 1967), alkali basalt (Stormer, 1972), and nephlinite

(Stormer, 1972), shown for comparison. Open triangles: alkali basalt;

open squares: tholeiitic basalt; solid triangles: nephlinite. (after

Stormer, 1972)
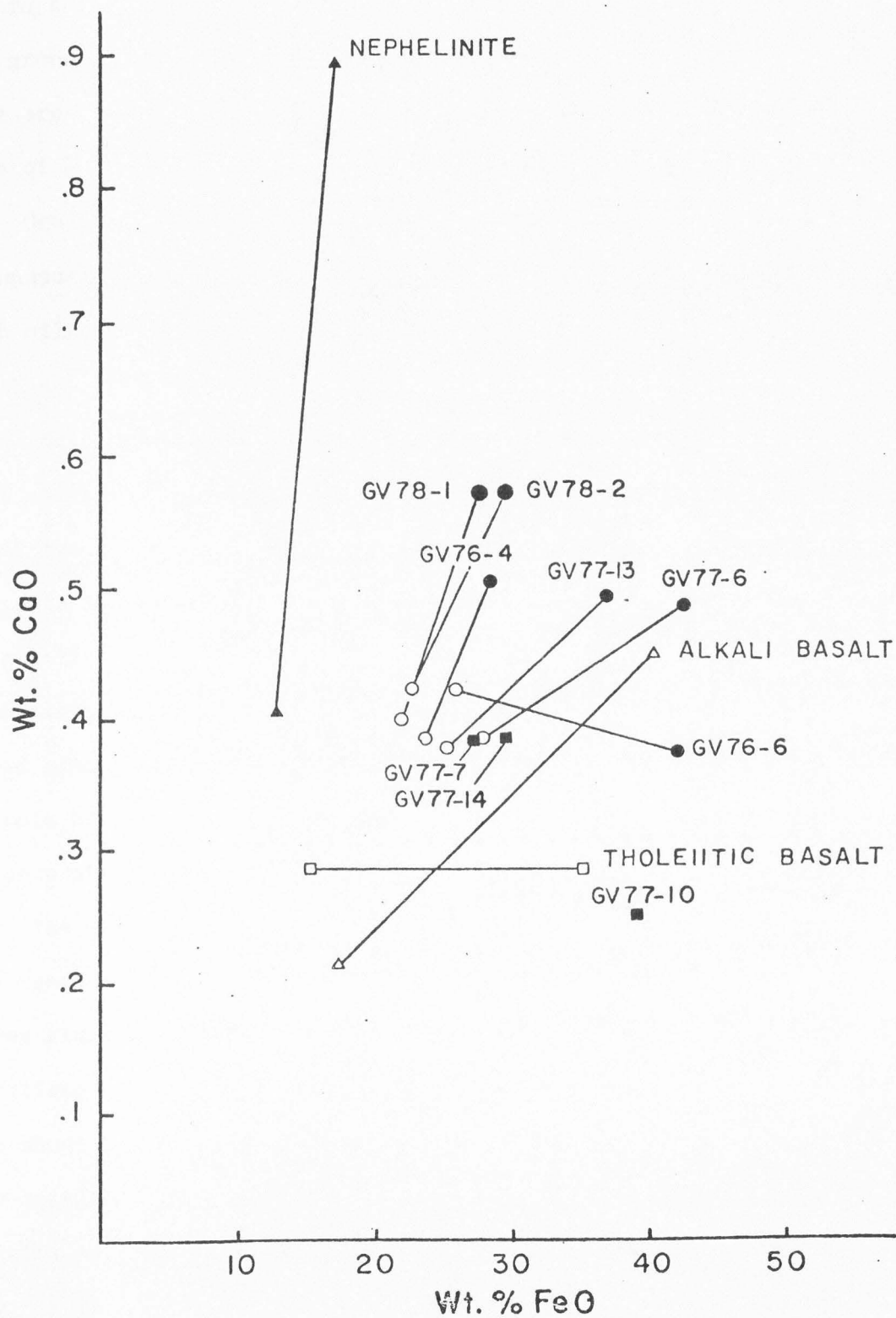
Due to the scarcity of olivine phenocrysts in the Group 2 basalts, only the groundmass was analyzed. Two samples (GV77-7, GV77-14) plot in the same area as the Group 1 phenocrysts. One sample (GV77-10) plots in an area of lower Ca and higher Fe than all other samples.

One sample from the Group 1 basalts (GV77-6) has what appears to be an unusually high iron content in the olivine without the correspondingly high silica content in the whole rock composition. The groundmass olivine in this sample has an average composition of Fo_{50} with the whole rock SiO_2 content of only 47 wt %. Carmichael et al. (1974) found that iron rich olivine (Fo_{50}) was confined to more siliceous lavas: trachytes and rhyolites. Stout and Nicholls (1977) also found olivines with high iron contents in basalts of the Snake River Plain, and suggested that this may be a reflection of the higher than average content of iron and the lower than average content of silica characteristic of the whole suite. This would also appear to apply to the Gem Valley basalts for they also contain higher than average amounts of iron and lower than average amounts of silica.

The olivine composition of the basalts of Gem Valley falls within the range of reported olivine compositions for basalts of the Snake River Plain (Stout and Nicholls, 1977; Leeman et al., 1976; Leeman and Vitaliano, 1976). The CaO and FeO contents of the Gem Valley basalts are about the same as the values reported by Stout and Nicholls (1977) for basalts of the Snake River Plain. The olivines of the Gem Valley basalts appear to be more extensively zoned than olivines of the McKinney Basalt reported by Leeman and Vitaliano (1976).

Pyroxene

Augite is present in the groundmass of all analyzed samples. However in only four samples (GV76-6, GV77-7, GV77-6, GV77-13) are the crystals large enough to permit microprobe analysis. Augite was detected in the remaining samples by x-ray diffraction techniques. No phenocrysts of pyroxene have been observed. Average microprobe analyses of augite are presented in Table 5.

Chemical variation of FeO, most extreme in GV77-6, is from 10.31 wt % to 17.53 wt % FeO. As with the plagioclase, this may also be a function of an environment of slower cooling in the interior of the lava flow. Least extensive variation with respect to FeO is in GV77-7, from 9.75 wt % to 11.85 wt % FeO. Average FeO content of all analyzed augite is 11.5 wt % FeO. Figure 12 illustrates pyroxene compositions with the Skaergaard trend for comparison.

The CaO content of the pyroxenes averages 19.9 wt %. Chemical variation with respect to CaO is again most extensive in GV77-6: 16.87 wt % to 21.67 wt %. In the remaining samples the variation does not exceed 3 wt % CaO. Iron enrichment occurs at the expense of both CaO and MgO in all samples. Minor elements (Ti, Mn, Na) show little variability in the analyzed samples. Titanium is the most variable with a range of 1 wt % TiO_2.

Kushiro (1960) and LeBas (1962) showed that aluminium content in clinopyroxenes may be used to determine magmatic parentage of the host rock. Clinopyroxenes from tholeiitic rocks contain the least amount of Al_2O_3, those from feldspathoid-free alkali rocks have more, and those of

Table 5: Average microprobe analyses of Gem Valley pyroxenes.

	GV76-6	GV77-6	GV77-7	GV77-13
SiO_2	48.47	49.61	49.41	48.79
TiO_2	2.02	1.73	1.93	1.51
Al_2O_3	3.92	2.70	4.73	2.88
FeO*	11.18	12.58	10.80	11.29
MnO	.25	.27	.31	.30
MgO	13.81	13.67	14.57	14.03
CaO	20.28	20.03	19.28	20.16
Na_2O	.40	.39	.40	.40
Total	100.33	100.98	101.43	99.36

*Total iron reported as FeO

Number of ions on the basis of 6 oxygens

	GV76-6	GV77-6	GV77-7	GV77-13
Si	1.8269	1.8654	1.8274	1.8580
Al^{IV}	.1731	.1198	.1726	.1295
Ti^{IV}	----	.0148	----	.0125
Al^{VI}	.0013	----	.0336	----
Ti^{VI}	.0573	.0342	.0538	.0308
Fe^{+2}	.3524	.3956	.3340	.3595
Mn	.0079	.0086	.0096	.0096
Mg	.7758	.7660	.8031	.7964
Ca	.8190	.8071	.7640	.8227
Na	.0294	.0285	.0289	.0298
Sum IV	2.0000	2.0000	2.0000	2.0000
Sum VI	2.0431	2.0400	2.0270	2.0488

Molecular percent

	GV76-6	GV77-6	GV77-7	GV77-13
Fs	18.07	20.09	18.44	17.56
En	39.60	38.70	39.32	42.06
Wo	42.33	41.20	42.24	40.37

Figure 12: Electron-microprobe analyses of augite plotted in terms of Ca-Fe-Mg. Large open circles show ranges for each sample; small solid circles show the average composition for each sample. Line illustrates calcium-rich trend of Skaergaard Complex pyroxenes (Brown and Vincent, 1963).

Di ———————————————————— Hd

Mg ———————————————————— Fe

GV76-6   GV77-6   GV77-13   GV77-7
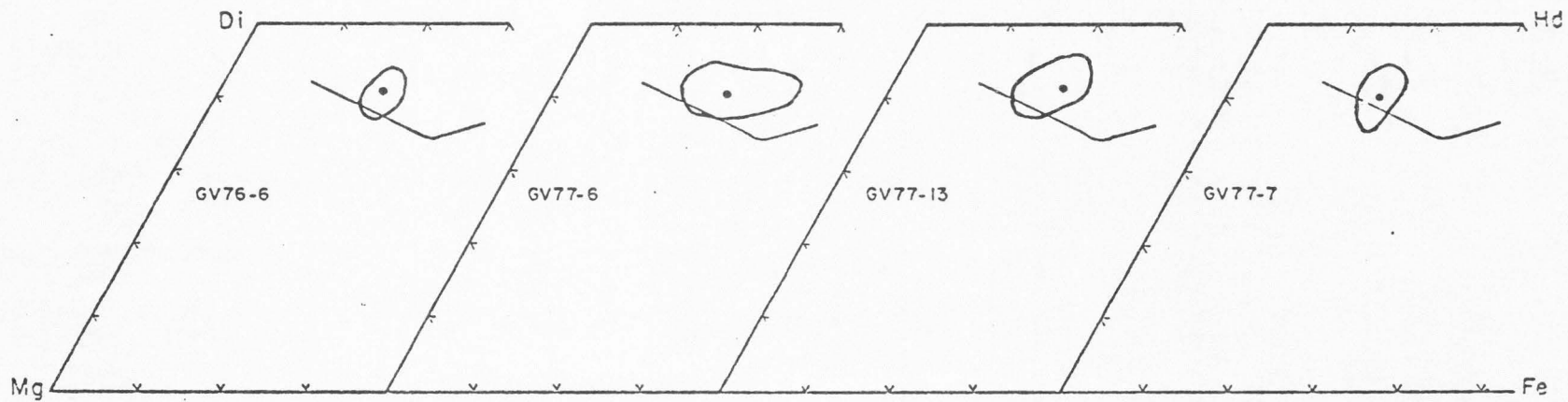
feldspathoid-bearing alkali rocks contain even greater amounts of Al_2O_3.
In a plot of silica versus alumina for many different magma types, LeBas
(1962) showed that there are three well-defined fields: (1) tholeiitic,
high-alumina, and calc-alkaline rocks; (2) normal-alkaline rocks; and (3)
peralkaline rocks. A plot of wt % SiO_2 versus wt % Al_2O_3 with the fields
defined by LeBas (1962) is shown in Figure 13. For comparison, fields
for the Kap Edvard Holm, Skaergaard Complex, and Snake River Plain have
been outlined. The graph shows the four Gem Valley augites are less
variable than the Snake River Plain and Kap Edvard Holm augites, but are
slightly more variable than the augites from the Skaergaard Complex.
Three of the Gem Valley pyroxenes plot in the normal alkaline field
whereas one (GV77-6) plots just over the boundary, in the tholeiitic
field.

Carmichael et al. (1974) demonstrated that lavas of low silica ac-
tivity will favor incorporation of Al in Z (tetrahedral) sites using the
following reaction:

$$CaAl_2SiO_6 + SiO_2 = CaAl_2Si_2O_8$$
pyroxene   glass anorthite
component
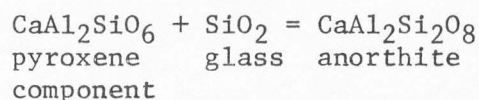
This reaction allows the division of magma types based on the proportion
of Z sites occupied by aluminum. In augite from olivine tholeiites only
2 % Al is found in the Z sites while up to 20 % may be found in the Z sites
of augites from lavas with lower silica activity. The Gem Valley basalts
range from 12 % to 17 % Al in the Z sites, averaging 15 % Al_z. LeBas (1962)
determined that an average of 90 % of the Al in pyroxene is in tetrahedral
coordination in the normal-alkaline series, whereas almost all the Al and
some Fe^{3+} and Ti are in tetrahedral coordination in peralkaline rocks.

Figure 13: Weight percent silica plotted against weight percent alumina for pyroxenes in the groundmass. Dashed lines separate fields defined by LeBas (1962): 1 = tholeiitic, high alumina, calc-alkaline; 2 = alkaline; 3 = peralkaline. Large open square: pyroxenes from the mildly alkaline Kap Edvard Holm intrusion (Elsdon, 1971); small lined square: pyroxenes of the Skaergaard Complex (Brown and Vincent, 1963); filled triangles and squares: pyroxenes of the Snake River Plain (Stout and Nicholls, 1977); filled circles: pyroxenes of the Gem Valley basalts.
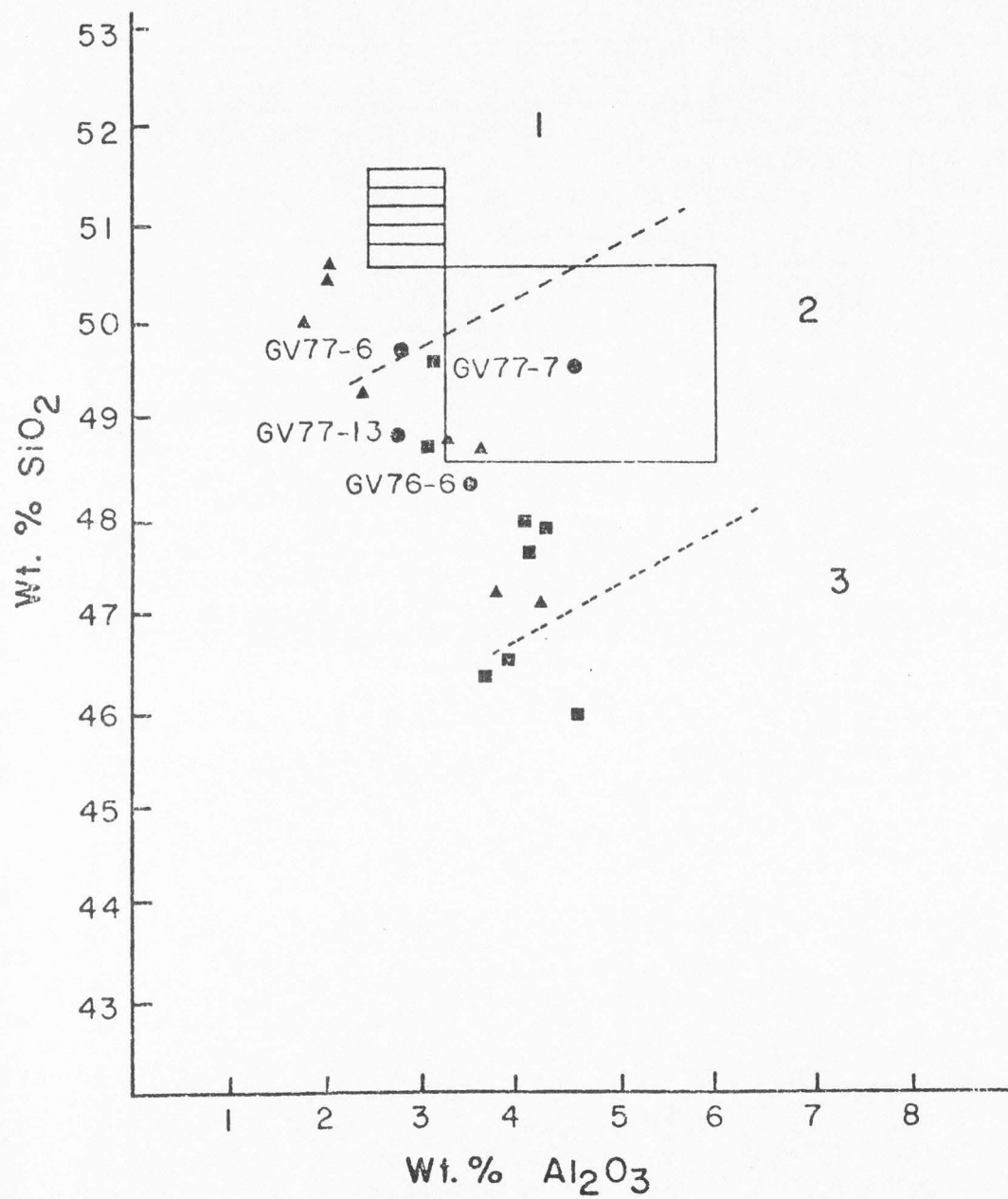
An average of 96 % of the Al is in tetrahedral coordination in the basalts from Gem Valley (range: 83%-100%).

Less than 1 wt % TiO_2 is found in pyroxenes from nonalkaline rocks whereas alkaline rock types contain more TiO_2 (LeBas, 1962). A plot of wt % TiO_2 versus Al_z in pyroxenes has been used by LeBas to differentiate nonalkaline, normal-alkaline, and peralkaline rock types (Figure 14). On this graph two samples of the basalts of the Gem Valley area plot in the normal-alkaline field and two samples plot just over the dividing line in the nonalkaline or tholeiitic field. The Gem Valley pyroxenes lie within or very near the field of basalts of the Snake River Plain.

The Na_2O content of pyroxenes of tholeiitic, high-alumina, and calc-alkaline rocks averages .35 wt % whereas that of pyroxenes of the normal-alkaline series averages .70 wt % (LeBas, 1962). The average Na_2O content in the Gem Valley pyroxenes is .40 wt % which is within the range of values (.31 wt % to .53 wt %) found in pyroxenes from basalts of the Snake River Plain (Stout and Nicholls, 1977).

The presence of only a high-calcium pyroxene, in the Gem Valley basalts, suggests an affinity to the alkali-olivine basalt suite. Normative nepheline is common to pyroxenes from alkali-olivine basalts and is present in the norms of three Gem Valley pyroxenes (GV76-6, GV77-6, GV77-13). Hypersthene is a common normative component in pyroxenes from tholeiitic basalts, and is present in the norm of one pyroxene from Gem Valley (GV77-7), although only in a very small amount. The normative compositions of pyroxenes of the Gem Valley area are given in Table 6. The method given by Powell and Powell (1974) was used in determining Fe^{3+}.

Figure 14: Plot of the percent Al_z versus weight percent TiO_2 for pyroxenes. Dashed lines separate fields defined by LeBas (1962): 1 = tholeiitic, high alumina calc-alkaline; 2 = alkaline; 3 = peralkaline. Large open square: pyroxenes of the Kap Edvard Holm intrusion (Elsdon, 1971); small lined square: pyroxenes of the Skaergaard Complex (Wager and Brown, 1967); large irregular oval: pyroxenes of the Snake River Plain (Stout and Nicholls, 1977).
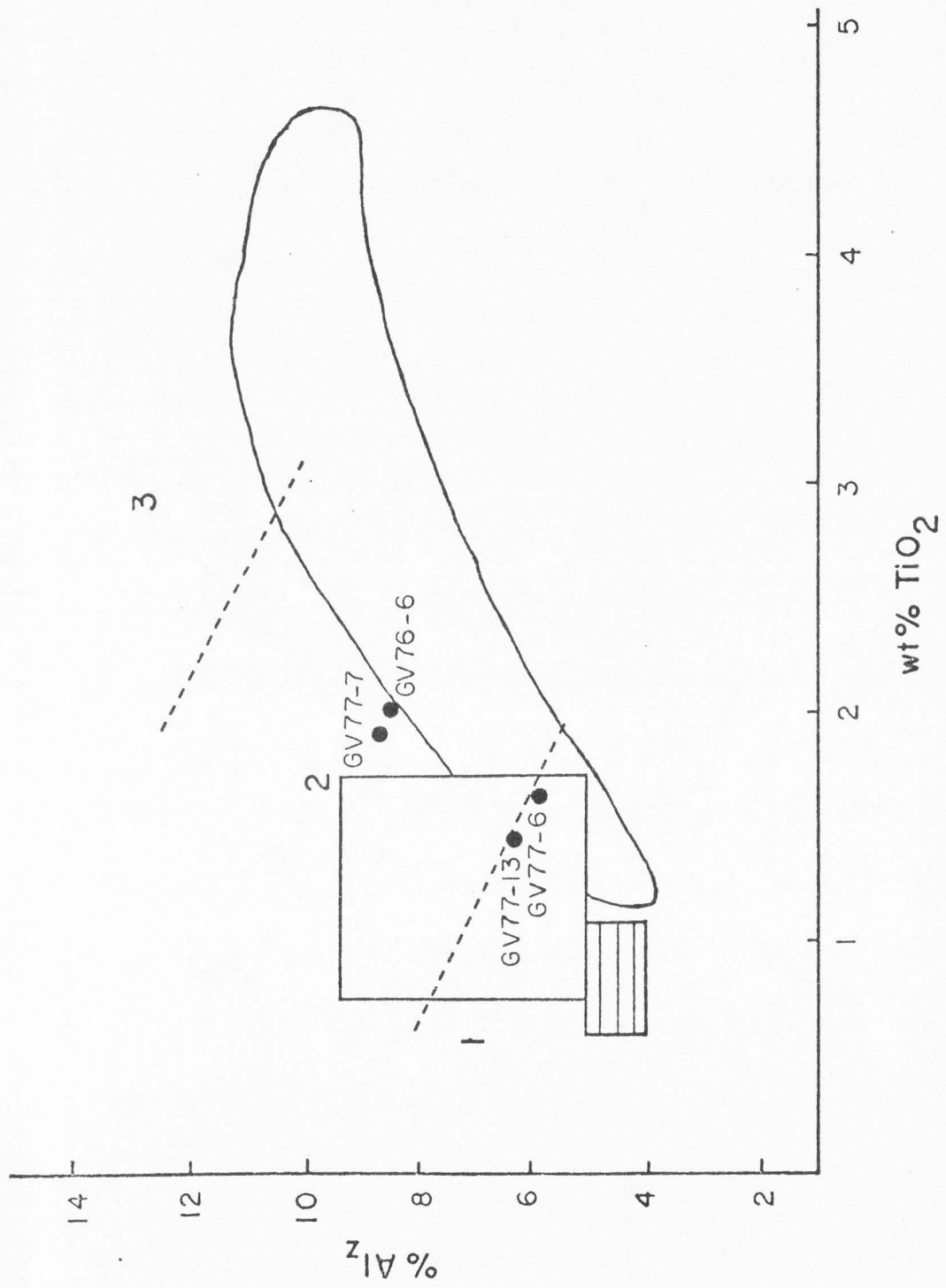
Table 6: Normative composition of the Gem Valley pyroxenes. (wt. %)

	GV76-6	GV77-6	GV77-13	GV77-7
Pl	8.90	7.16	6.54	14.50
(Ab)	----	1.54	.48	3.38
(An)	8.90	5.62	6.06	11.12
Ne	1.83	.95	1.57	----
Di	73.65	77.43	76.22	68.35
(Wo)	37.95	39.70	39.23	35.30
(En)	23.59	23.44	24.06	22.41
(Fs)	12.11	14.29	12.94	10.64
Hy	----	----	----	.42
(En)	----	----	----	.28
(Fs)	----	----	----	.13
Ol	11.86	12.42	12.15	14.51
(Fo)	7.57	7.43	7.63	9.53
(Fa)	4.29	4.99	4.52	4.98
Cs	.25	----	----	----
Il	3.84	3.29	2.87	3.67
Total	100.33	101.25	99.36	101.43

Orthopyroxene Xenocryst

The orthopyroxene xenocryst in GV78-8 was analyzed. The results of the analysis are presented in Table 7. The olivine and augite in the reaction rim surrounding the orthopyroxene were also analyzed. The results of these analyses are also presented in Table 7. Due to the limited abundance and very fine-grained nature of the augite in the reaction rim only a partial analysis was completed. The orthopyroxene composition was found to average En_{71}. In the surrounding rim the augite has an average composition of $En_{45}Fs_{20}Wo_{35}$. The average composition of the olivine in the rim is Fo_{60} which is within the range of the groundmass olivine found in GV77-14, also from King Canyon.

The presence of a reaction rim surrounding the orthopyroxene indicates that the xenocryst was not in equilibrium with the host rock. Kuno (1950) observed orthopyroxene with rims containing olivine and augite in olivine-augite basalts from Hakone volcano in Japan. He suggested the instability of the orthopyroxene was due to its xenocrystal character and hence, it is unstable in the melt. Formation of the olivine rim must have occurred when the magma was at a temperature lower than the liquidus temperature of the xenocryst. At temperatures above the liquidus temperature the xenocryst would melt. The reaction of the xenocryst with the silica-poor iron-rich liquid may produce the olivine rim by driving the following reaction to the left:

$$(Mg,Fe)_2SiO_4 + SiO_2 = 2(Mg,Fe)SiO_3$$

$$\text{olivine} \qquad\qquad\qquad \text{orthopyroxene}$$
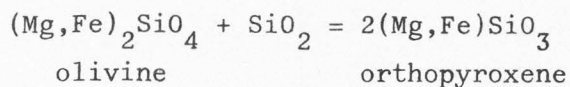
Table 7: Microprobe analyses of xenocryst, olivine in the xenocryst
rim, and partial analyses of augite in the xenocryst rim
rim of sample GV77-8.

	Xenocryst Enstatite	Xenocryst Rim Olivine	Augite
SiO_2	52.53	35.30	----
TiO_2	.57	.05	----
Al_2O_3	3.14	.24	----
FeO	16.70	34.48	12.06
MnO	.38	.60	----
MgO	23.83	26.59	15.00
CaO	1.76	.34	16.10
Na_2O	.09	1.10	----
Total	99.00	98.70	43.16
	Mol %	Mol %	Mol %
	En 71	Fo 60	En 45
	Fs 26	Fa 40	Fs 20
	Wo 3		Wo 35

Fe-Ti Oxides

Both magnetite and ilmenite are present in every sample except
GV77-14, where magnetite is the only Fe-Ti oxide present. In most
samples magnetite has undergone exsolution to form either intergrowths
of ilmenite and magnetite or compound grains of magnetite and ilmenite.
Three samples (GV76-6, GV76-4, GV77-14) contain magnetites which are
homogeneous and their analyses are presented in Table 8. Ilmenite is
found as discrete lath shaped or tabular crystals in three samples
(GV76-4, GV76-6, GV77-6). However, due to the exsolution of the magne-
tite, the ilmenite in GV77-6 was not analyzed. Analyses of the ilmenite
in GV76-4 and GV76-6 are presented in Table 8. Molecular end members for
the ilmenite-hematite (il-hm or α) solid solution series and the magne-
tite-ulvospinel (mt-usp or β) solid solution series were calculated
according to the method given by Carmichael (1967a).

Carmichael (1967a) noted a relationship between the composition of
the oxide phases present and the coexisting ferromagnesian silicates.
When associated with olivine and augite the β phase is approximately
65-74 mol % usp (Smith and Carmichael, 1968) whereas the α phase is
approximately 4-6 mol % hm (Carmichael, 1967b). The analyzed magnetites
range between usp_{52} and usp_{66} whereas the ilmenites have compositions
between hm_9 and hm_{12}. The range of compositions of the magnetites and
ilmenites is similar to that reported by Stout and Nicholls (1977) for
the Snake River Plain (5-11 mol % hm; 58-74 mol % usp).

Magnetites found in lavas with low silica activity usually contain
more Al_2O_3 and MgO than magnetites found in tholeiitic lavas (Carmichael

Table 8: Average microprobe analyses of magnetite and ilmenite.

Magnetite

	GV76-4	GV76-6	GV77-14
SiO_2	.51	.37	.37
TiO_2	23.28	18.50	22.17
Al_2O_3	2.19	1.92	3.55
V_2O_3	.78	1.18	.71
Cr_2O_3	.29	.25	.04
FeO	68.28	72.82	68.33
MnO	.59	.42	.50
MgO	1.75	1.61	2.64
CaO	.41	.23	.19
ZnO	.02	.03	.02
Sum	98.09	97.36	98.52
Fe_2O_3	20.30	29.81	22.36
FeO	50.02	45.99	48.21
Total	100.13	100.32	100.76

Molecular Fractions

	GV76-4	GV76-6	GV77-14
Magnetite	.3418	.4750	.3880
Ulvospinel	.6582	.5250	.6120

Ilmenite

	GV76-4	GV76-6
SiO_2	1.30	.37
TiO_2	45.30	48.60
Al_2O_3	1.49	.31
V_2O_3	.13	.33
Cr_2O_3	.02	.11
FeO	47.31	46.30
MnO	.65	.54
MgO	1.36	2.83
CaO	.63	.35
ZnO	.35	.26
Sum	98.55	100.00
Fe_2O_3	10.24	9.36
FeO	38.09	37.88
Total	99.57	100.94

Molecular Fractions

	GV76-4	GV76-6
Ilmenite	.8807	.9049
Hematite	.1193	.0951

et al., 1974). The magnetites in alkali-olivine basalts typically contain 3-5 wt % Al_2O_3 and 1-3 wt % MgO compared to 1-2 wt % Al_2O_3 and 0.5-1.5 wt % MgO for magnetites in tholeiitic basalts. Analyses of magnetites in basalts of the Gem Valley area reveal that one sample, GV77-14, is within the range for alkali-olivine basalt and two samples, GV76-4 and GV76-6, have compositions more closely allied with tholeiitic basalts.

CHEMISTRY AND CLASSIFICATION

Chemical analyses were conducted using the methods presented by Carmichael et al. (1968). Results of the chemical analyses and the CIPW norms are presented in Table 9.

The basaltic lavas of the Gem Valley area have SiO_2 contents ranging from 45 wt % to 48 wt % which is within the range of silica contents found in basalts from the Snake River Plain (Stout and Nicholls, 1977; Leeman and Vitaliano, 1976; Leeman et al., 1976; Leeman and Rogers, 1970). Powers (1960), in a triangular plot of silica, magnesia, and total iron plus manganese from whole-rock analyses, found basalts of the Snake River Plain to be lower in silica and richer in iron than basalts from the Columbia River area and the Cascade Range. On Powers' triangular diagram, the Group 1 basalts plot in the field of the basalts of the Snake River Plain (Figure 15). However, the Group 2 basalts (with GV77-7 omitted because of oxidation) plot in the field of the Columbia River basalts. This reflects the lower MgO content of the Group 2 basalts.

Differences in the major oxide compositions of the Group 1 and the Group 2 basalts appear in the amounts of Na_2O, MgO, Al_2O_3, and total iron. The Group 1 basalts are higher in MgO and total iron whereas the Group 2 basalts are higher in Na_2O and Al_2O_3. The higher MgO and total iron content of the Group 1 basalts may be a reflection of the higher modal olivine present in these basalts (Table 2). The higher Na_2O content of the Group 2 basalts would appear to be a reflection of the more sodic composition of the plagioclase. Also, the higher Na_2O and Al_2O_3 contents of

Table 9: Chemical analyses and CIPW norms of the basalts

from the Gem Valley area.

	Group 1						Group 2		
	Sample numbers						Sample numbers		
	GV76-4	GV76-6	GV77-6	GV77-13	GV78-1	GV78-2(glass)	GV77-7	GV77-10	GV77-14
SiO_2	46.87	47.53	47.08	46.09	47.60	45.25	45.63	47.21	47.77
TiO_2	3.07	2.47	2.83	3.12	2.35	3.77	3.97	2.87	2.78
Al_2O_3	14.85	15.43	14.80	14.49	15.62	12.39	13.15	17.67	17.89
Fe_2O_3	2.34	1.68	2.65	6.18	1.52	*	10.38	6.01	3.15
FeO	11.56	11.03	10.74	8.57	10.56	15.75	5.76	6.00	8.72
MnO	.22	.22	.19	.23	.18	.31	.24	.20	.19
MgO	6.58	6.69	6.65	6.41	6.60	6.83	5.22	3.77	4.00
CaO	9.29	9.78	9.95	9.53	9.68	10.18	8.93	9.79	9.56
Na_2O	2.89	2.92	2.93	2.79	2.62	2.64	3.12	3.37	3.32
K_2O	1.09	1.25	.80	.98	1.38	1.26	1.37	1.38	1.17
P_2O_5	.79	.57	.56	.91	.52	---	1.17	.92	.79
H_2O^+	.46	.26	.70	.42	.64	---	.62	.36	.27
H_2O^-	.09	.04	.00	.03	.05	---	.11	.06	.15
Total	100.10	99.87	99.88	99.75	99.32	98.38	99.67	99.61	99.76
qt	---	---	---	---	---	---	2.69	.48	---
or	6.44	7.39	4.73	5.79	8.15	7.45	8.10	8.15	6.91
pl	48.78	50.01	49.66	47.73	48.96	32.61	44.23	57.53	58.55
(ab)	24.45	24.71	24.79	23.61	22.17	14.37	26.40	28.52	28.09
(an)	24.33	25.30	24.87	24.12	26.79	18.24	17.83	29.01	30.46
ne	---	---	---	---	---	4.31	---	---	---
di	13.68	16.08	17.09	13.83	14.70	26.98	14.64	10.73	9.74
(wo)	6.93	8.14	8.69	7.19	7.45	13.47	7.86	5.66	4.93
(en)	3.57	4.15	4.67	4.85	3.84	5.70	6.79	4.30	2.51
(fs)	3.18	3.79	3.73	1.79	3.41	7.80	---	.77	2.31
hy	6.64	.26	5.69	14.26	5.60	---	6.21	6.00	7.27
(en)	3.51	.14	3.16	10.41	2.96	---	6.21	5.09	3.79
(fs)	3.13	.12	2.53	3.85	2.63	---	---	.91	3.49
ol	12.95	17.39	11.50	.70	13.35	19.87	---	---	5.18
(fo)	6.52	8.67	6.12	.50	6.75	7.92	---	---	2.57
(fa)	6.42	8.72	5.38	.20	6.60	11.95	---	---	2.61
mt	3.39	2.44	3.83	8.96	2.20	---	7.87	8.71	4.57
il	5.83	4.69	5.37	5.93	4.46	7.16	7.53	5.45	5.28
ap	1.87	1.35	1.34	2.16	1.23	---	2.78	2.18	1.87
Total	99.59	99.60	99.21	99.35	98.66	98.38	99.00**	99.24	99.38
Salic	55.22	57.40	54.39	53.52	57.11	44.37	55.02	66.16	65.46
Femic	44.37	42.20	44.82	45.83	41.55	54.01	43.98	33.07	33.92
Differentiation Index	30.90	32.09	29.52	29.40	30.32	26.13	37.19	37.15	35.01

* Total iron analyzed as FeO
** Total includes 4.95 % normative hematite

Figure 15: Triangular plot of SiO_2, MgO, and ($FeO+Fe_2O_3+MnO$) for basalts from the northwestern United States. Shaded area of inset shows relative position of large triangle in the ternary diagram. Vertically lined area: basalts of the Cascades (CAS); horizontally lined area: basalts of the Columbia River Plateau (CRP); open irregular field: basalts of the Snake River Plain (SRP); filled circles: basalts of the Gem Valley area. All data plotted in terms of weight percent recalculated to 100% (after Powers, 1960).
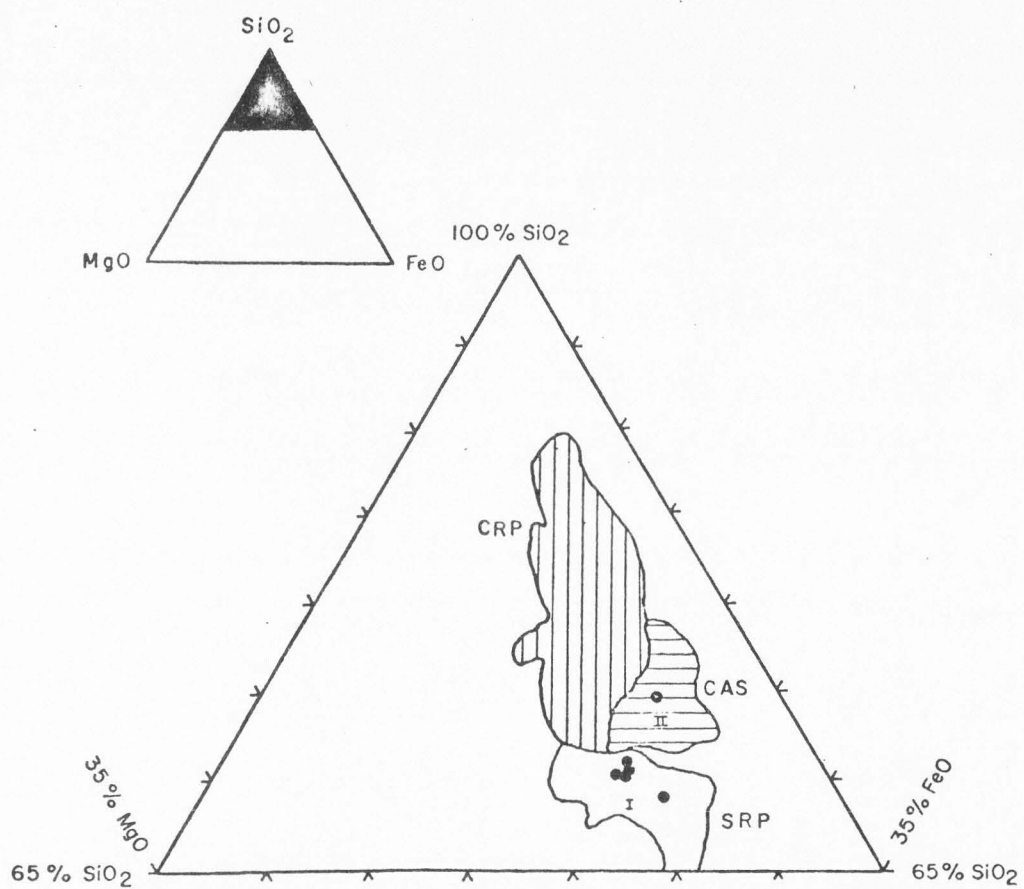
the Group 2 basalts may indicate the presence of unidentified plagio-
clase in the groundmass which is masked by the opaques or too fine grained
for identification. The remaining oxides of both groups are similar.
When compared to the basalts of the Snake River Plain, the basalts of the
Gem Valley area are generally lower in MgO and higher in Al_2O_3. The re-
maining oxides are present in amounts comparable to the basalts of the
Snake River Plain.

MacDonald and Katsura (1964) were able to distinguish alkali-olivine
basalts and tholeiitic basalts of Hawaii on an alkali-silica variation
diagram. Figure 16 shows that all of the Gem Valley area basalts lie in
the field of alkali-olivine basalt, well above the line dividing tholeiitic
and alkali-olivine basalts.

The CIPW norms show olivine occurring in amounts up to 20 wt %.
Hypersthene is also present in a wide range from .2 wt % to 18 wt %. Two
samples, GV77-7 and GV77-10, have quartz present in the norm. However,
the presence of quartz appears to be controlled by the degree of oxidation
of these samples. This is reflected in the amount of Fe_2O_3 present in the
bulk-rock analyses. If the amount of Fe_2O_3 exceeds the amount of FeO
present, there will be insufficient FeO remaining to produce olivine in
the norm calculations. This leads to excess silica and therefore quartz
in the norm. The presence of hypersthene and olivine and the absence of
nepheline, in the norm, suggests that these basalts are olivine tholeiites
(Yoder and Tilley, 1962). However, like basalts of the Snake River Plain,
their modal mineralogy suggests affinity to the alkali-olivine basalts
because of the presence of olivine and only one pyroxene, augite. Also
presented in Table 9 is the analysis of the residual glass found in a
pillow basalt (GV78-2). The glass was found to be nepheline normative

Figure 16: Alkali-silica variation diagram. Fields for tholeiitic and alkali-olivine basalts defined by MacDonald and Katsura (1964) for Hawaiian lavas. Filled circles: Group 1 lavas; filled squares: Group 2 lavas.
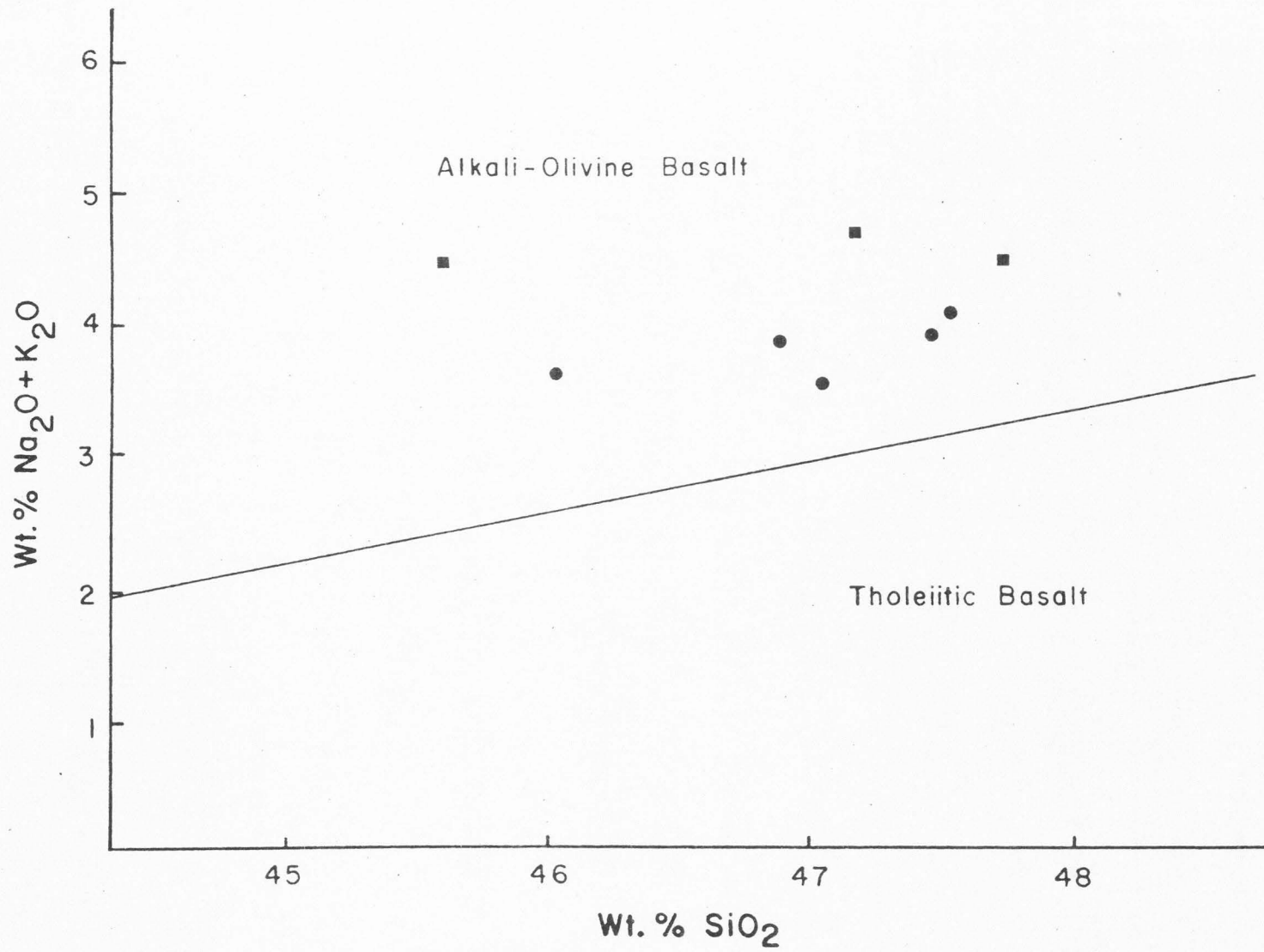
which classifies it as an alkali-olivine basalt. This is in contrast to the whole-rock analysis of a pillow basalt (GV78-1) which is hypersthene normative and would be classified as an olivine tholeiite.

Thornton and Tuttle (1960) defined the differentiation index (DI) as the sum of the normative salic components. This index is a widely used indicator of magmatic evolution. The DI of the Group 1 basalts averages 30, whereas the DI of the Group 2 basalts averages 36. This suggests that the Group 2 basalts are more differentiated than the Group 1 basalts. Stout and Nicholls (1977) reported that the DI of basalts of the Snake River Plain ranges from 24 to 29, whereas the DI of the basalts of the Craters of the Moon is 40.

Coombs (1963) formulated an indicator ratio, based on normative hypersthene, diopside, and quartz, that shows the degree of alkalinity and a projected course of differentiation. Basalts of the Gem Valley area are plotted on the Di - Ol - Qz - Ne tetrahedron of Coombs (1963) in Figure 17. Most basalts of the Gem Valley area lie in the mildly alkaline and transitional field. Coombs (1963) found that an indicator ratio of 0.00 to 0.38 is characteristic of mildly alkaline and transitional basalts. The range of indicator ratios for the basalts of the Gem Valley area is 0.01 to 0.35. Most alkaline suites having nepheline in the norm give an indicator ratio of less than zero. With an indicator ratio of less than 0.5, hypersthene is unlikely to appear during crystallization. As the indicator ratio approaches zero, olivine and augite crystallize simultaneously. This appears to be consistent with the observed mineralogy in the basalts of the Gem Valley area, that is, the presence of coexisting olivine and augite in the groundmass but no Ca-poor pyroxene.

Figure 17: Compositions of the Gem Valley basalts plotted on a nepheline (Ne) - diopside (Di) - olivine (Ol) - quartz (Qz) diagram with fields as determined by Coombs (1963). All samples plotted in terms of normative Ne, Di, Hy, and Qz recalculated to 100%.

NaAlSiO₄ → ... (figure, ternary diagram)
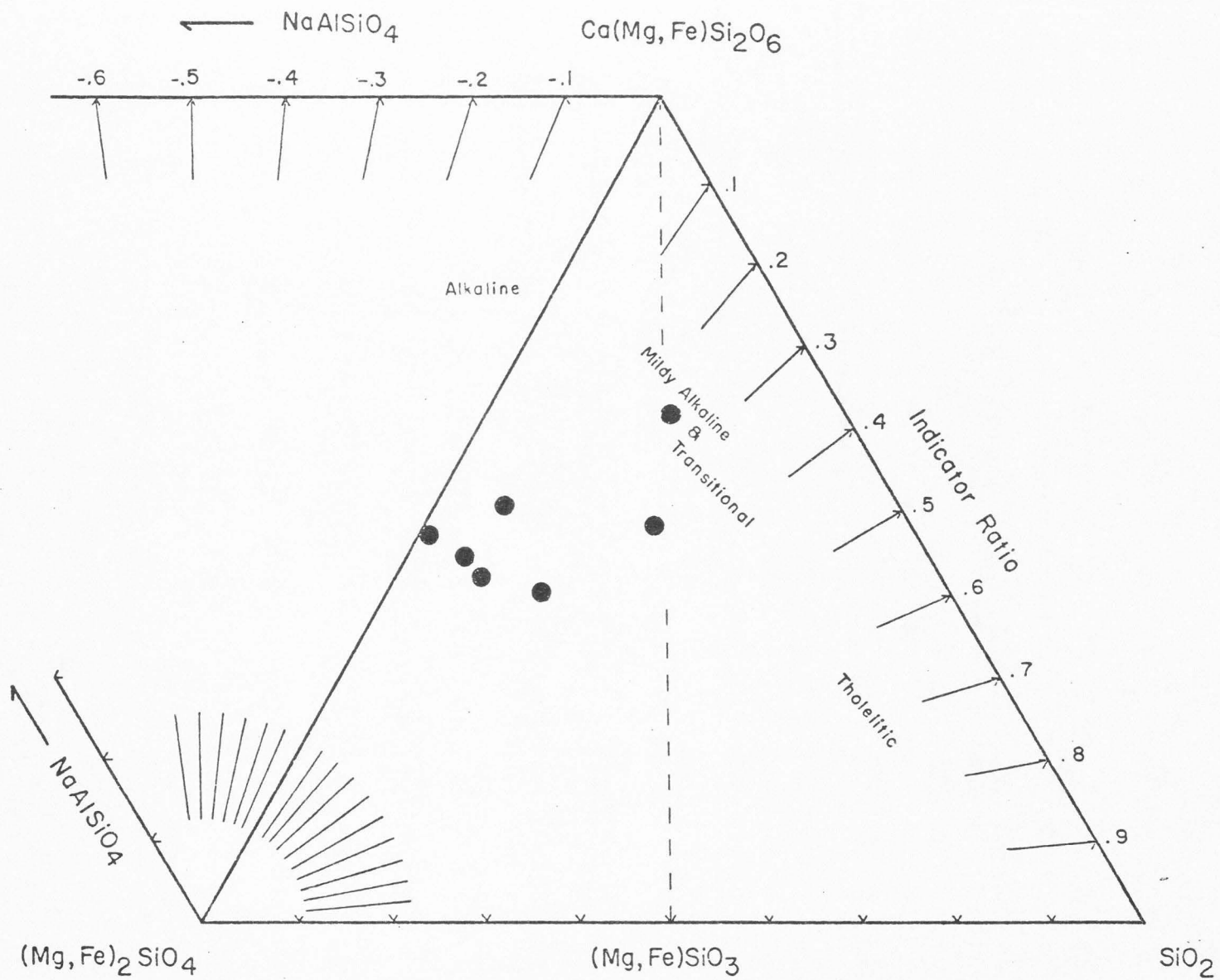
A study by Muan and Osborn (1956) indicated the importance of the partial pressure of oxygen in determining the direction of change in the compositions of liquids during crystallization. Two different courses of crystallization were observed in iron-oxide systems depending on which remains constant, the total composition of the mixture or the partial pressure of oxygen. Osborn (1959) illustrated these trends for fractionally crystallized liquids on a plot of $(FeO+Fe_2O_3)/(FeO+Fe_2O_3+MgO)$ versus SiO_2. Three curves in Figure 18 show possible courses of fractionally crystallized liquids under conditions of: (1) constant total composition, curve A; (2) constant P_{O_2}, curve B; (3) increasing P_{O_2} from .21 atm to 1.0 atm, curve C, (Osborn, 1959). Also shown are curves representing trends of lavas from Thingmuli, the Skaergaard Complex, and the Cascade Range (Carmichael, 1964). The trends illustrated by Thingmuli and Skaergaard appear to follow that of a liquid fractionating at constant composition at the early stages of crystallization. The Cascade trend, in contrast, appears to follow a path of constant P_{O_2}. Stout and Nicholls (1977) illustrated the similarity of the trends of the basalts of the Snake River Plain to that of the Skaergaard Complex. The basalts of Group 1 and Group 2 also approximate the Skaergaard trend and are seen to separate on this plot much like basalts of the Craters of the Moon and the Snake River Plain.

A similarity of the trends toward iron enrichment is also observed by plotting basalts of the Snake River Plain, the Skaergaard Complex, Thingmuli, and the Gem Valley area on a triangular AFM diagram (Figure 19). Again there is a separation between the Group 1 and the Group 2 basalts, although it is not to the degree as that exhibited by basalts of the Snake River Plain and the Craters of the Moon.

Figure 18: The ratio of $(FeO+Fe_2O_3)/(FeO+Fe_2O_3+MgO)$ versus weight percent silica. Curves representing Skaergaard, Thingmuli, and the Cascades shown for comparison (after Carmichael, 1964). Curve A: constant total composition; curve B: constant partial pressure of oxygen; curve C: increasing partial pressure of oxygen (Osborn, 1959). Open squares: basalts from the Snake River Plain (SRP) and Craters of the Moon (COM) (Stout and Nicholls, 1977); filled circles: Group 1 basalts; filled squares: Group 2 basalts.

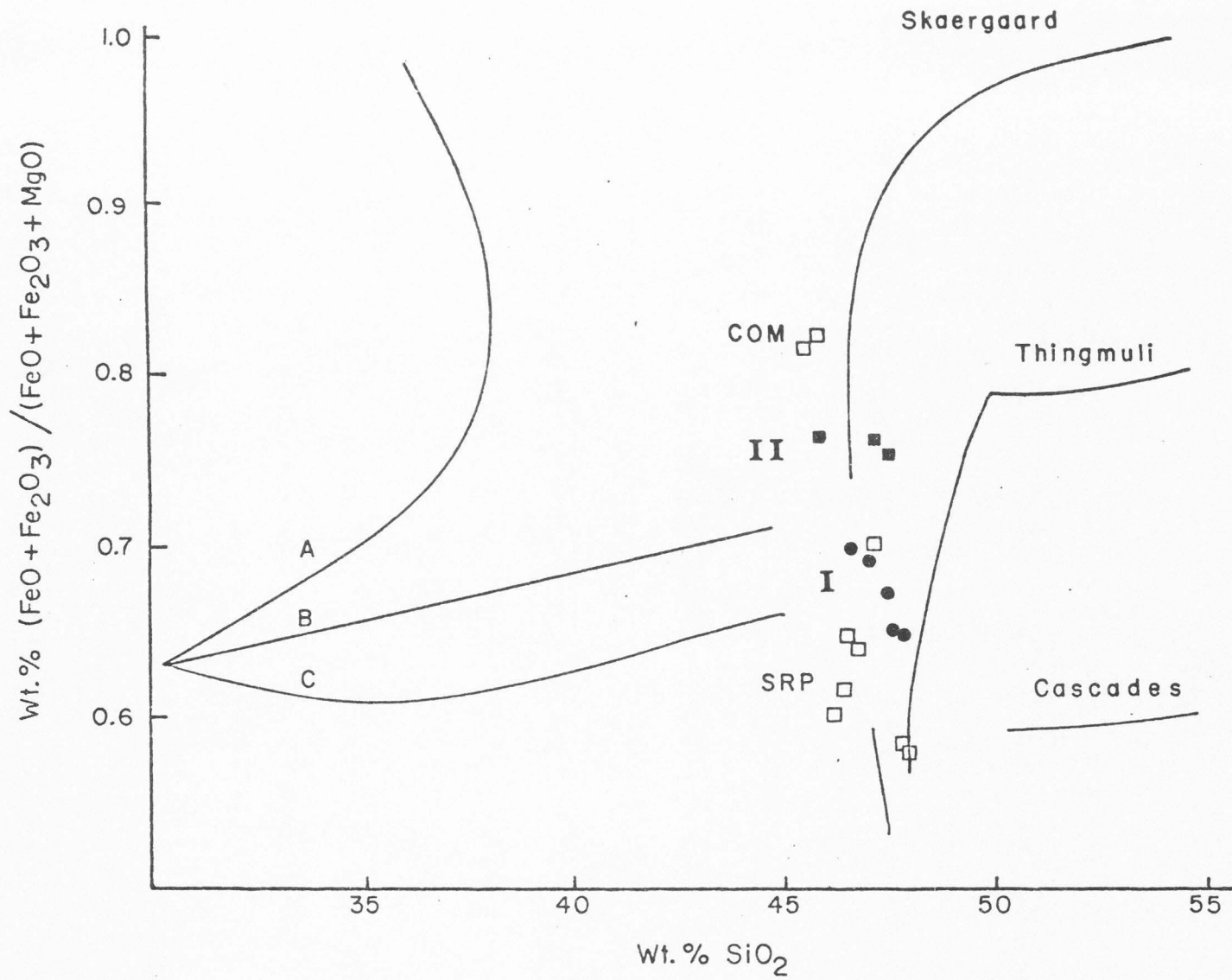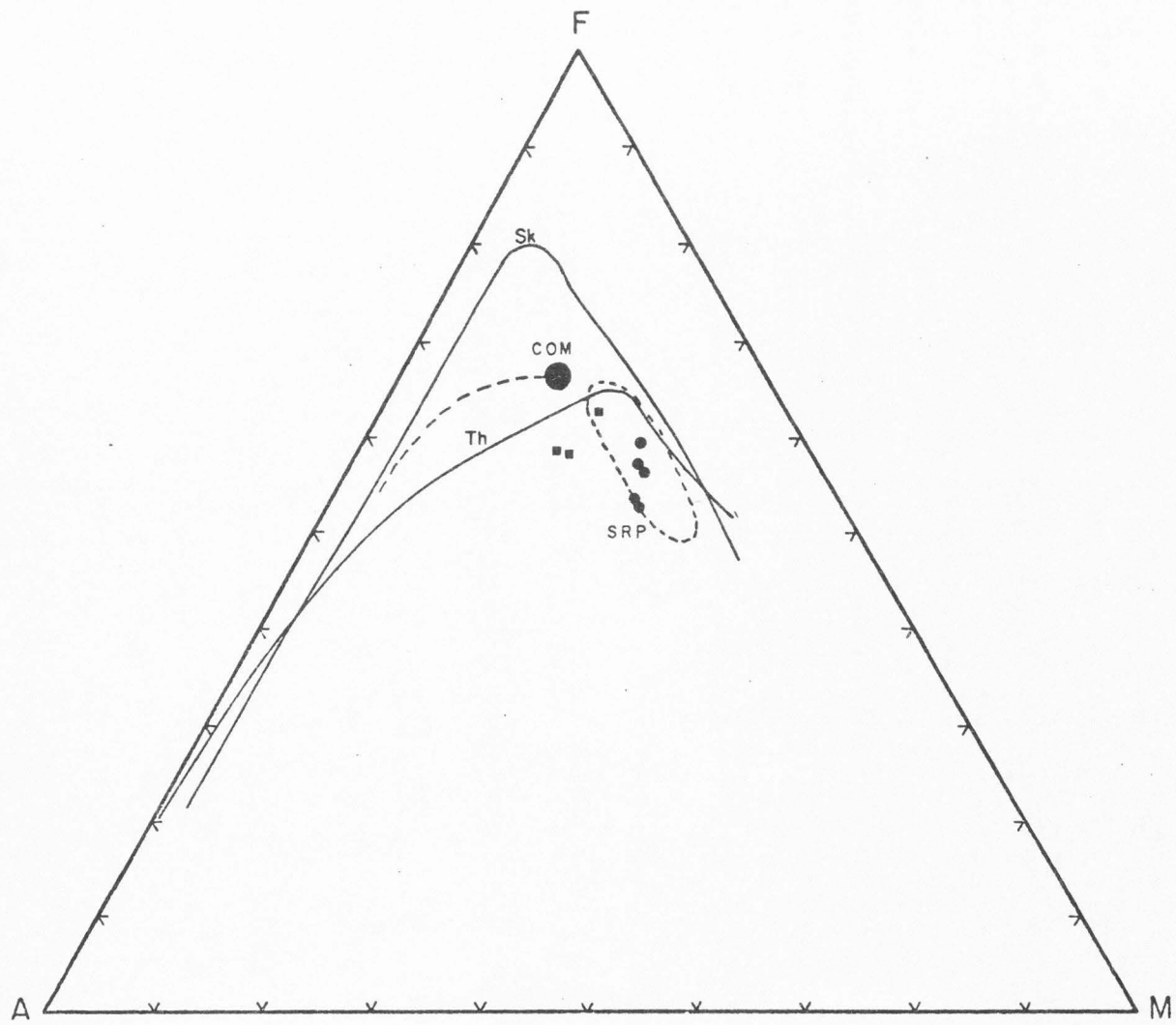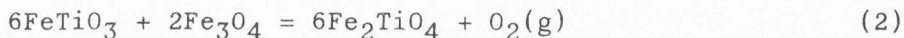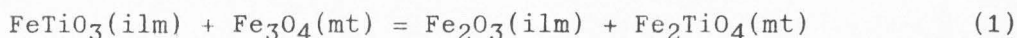Figure 19: AFM diagram for alkali, iron, and magnesium in basalts of the Gem Valley area. Filled circles: Group 1 basalts; filled squares: Group 2 basalts. Skaergaard (Sk) and Thingmuli (Th) trends are from Carmichael (1964). Snake River Plain trend (dashed line) and basalt field (SRP) are from Leeman et al. (1976). Basalts from Craters of the Moon (COM) are from Stout and Nicholls (1977).

PETROLOGY AND PETROGENESIS

Temperatures of Crystallization

The presence of coexisting magnetite and ilmenite allows the calcu-
lation of temperatures and oxygen fugacities in two samples (GV76-4 and
GV76-6). The geothermometers of Buddington and Lindsley (1964) and
Powell and Powell (1977) were used. Both methods are based on solid
solutions of magnetite-ulvospinel and ilmenite-hematite. Buddington
and Lindsley (1964) presented their data graphically with temperatures
and oxygen fugacities determined by the intersections of curves repre-
senting the mole fractions of magnetite ($X_{Fe_3O_4}$) and ilmenite (X_{FeTiO_3}).
Powell and Powell (1977) reformulated the geothermometer of Buddington
and Lindsley (1964) on a thermodynamic basis using the following reac-
tions:

$$FeTiO_3(ilm) + Fe_3O_4(mt) = Fe_2O_3(ilm) + Fe_2TiO_4(mt) \qquad (1)$$

$$6FeTiO_3 + 2Fe_3O_4 = 6Fe_2TiO_4 + O_2(g) \qquad (2)$$

Reaction 1 is independent of oxygen and the temperature calculation is
derived from the equilibrium relation:

$$-\Delta G_1^O = RTln(a_{Fe_2TiO_4,mt} \cdot a_{Fe_2O_3,ilm})/(a_{Fe_3O_4,mt} \cdot a_{FeTiO_3,ilm}) \qquad (1a)$$

Using reaction 2 the fugacity of oxygen calculation is derived from the
equilibrium relation:

$$-\Delta G_2^O = RTln(a^6_{Fe_2TiO_4,mt})/(a^6_{FeTiO_3,ilm} \cdot a^2_{Fe_3O_4,mt}) + RTln\ f_{O_2} \qquad (2a)$$

The graphical method assumes that coexisting Fe-Ti oxides do not
depart from the system $FeO-Fe_2O_3-TiO_2$ (Powell and Powell, 1977). When
this is true, the error in the graphically determined temperature is

$\pm$ 30°C and the error in oxygen fugacity (ln f_{O_2}) is ±2 (Buddington and
Lindsley, 1964). The thermodynamic approach of Powell and Powell (1977)
allows for the departure from the FeO-Fe_2O_3-TiO_2 system and calculates
appropriate maximum and minimum temperatures and oxygen fugacities for
each magnetite-ilmenite pair. Temperatures and oxygen fugacities deter-
mined by both methods are presented in Table 10. The two methods are in
agreement in that the temperature and oxygen fugacity determined graph-
ically (Buddington and Lindsley, 1964) are within the range of values
(GV76-4: 1294°C-1040°C, -14.3--23.1; GV76-6: 929°C-1032°C, -22.6--27.0)
calculated using the method of Powell and Powell (1977). It may also be
noted that the range of values for temperature and oxygen fugacity are
greater in GV76-4 than the range of values for GV76-6. This is due to
the increased Al_2O_3 and MgO in the magnetite and increased Al_2O_3 in the
ilmenite of sample GV76-4. The greater the compositional variation of
the magnetite-ilmenite pair from the FeO-Fe_2O_3-TiO_2 system, the greater
the uncertainties in the calculated temperatures and oxygen fugacities
(Powell and Powell, 1977).

The presence of coexisting olivine and pyroxene in the groundmass
of four samples (GV76-6, GV77-7, GV77-6, GV77-13) allows the calculation
of temperatures using the olivine-clinopyroxene geothermometer (Powell
and Powell, 1974). The following iron-magnesium exchange reaction be-
tween olivine and calcium-rich clinopyroxene is the basis for this geo-
thermometer:

$$2CaMgSi_2O_6 + Fe_2SiO_4 = 2CaFeSi_2O_6 + Mg_2SiO_4 \qquad (3)$$
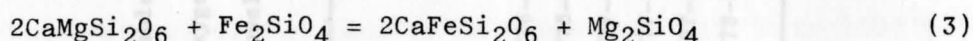
The calculated temperatures range from 1000°C for sample GV77-6 to
1016°C for sample GV77-7 (Table 10). A comparison of the olivine-clino-
pyroxene temperature with the magnetite-ilmenite temperatures is possible

Table 10: Temperatures of crystallization for basalts from the Gem Valley area. Average temperatures and
oxygen fugacities reported for the Mt - Il geothermometers of Buddington and Lindsley (1964) and Powell and
Powell (1977).

| | Mt - Il (Buddington & Lindsley) | | Mt - Il (Powell & Powell) | | Ol - Cpx (Powell & Powell) | Plag - Glass (Kudo & Weill) | Plag - Glass (Mathez) |
	T^oC	$\ln f_{O_2}$	T^oC	$\ln f_{O_2}$	T^oC	T^oC	T^oC
GV76-4	1090	-21	1167	-19	X	X	X
GV76-6	958	-26	981	-25	1002	X	X
GV77-6	X	X	X	X	1000	X	X
GV77-7	X	X	X	X	1016	X	X
GV77-13	X	X	X	X	1005	X	X
GV78-2	X	X	X	X	X	1240	1185

only for sample GV76-6. At a pressure of 1 bar, the calculated

olivine-clinopyroxene temperature of crystallization is $1002^{\circ}C$, within

the range of temperatures ($929^{\circ}C$-$1032^{\circ}C$) indicated using the magnetite-

ilmenite geothermometer of Powell and Powell (1977). The olivine-clino-

pyroxene temperature is not within the $\pm30^{\circ}C$ range of the magnetite-

ilmenite geothermometer of Buddington and Lindsley (1964). However,

this may be due to the lesser amounts of Al_2O_3 and MgO present in the

magnetite and Al_2O_3 in the ilmenite of sample GV76-6.

The coexisting plagioclase and glass present in GV78-2 permit the

calculation of temperature using both the Kudo and Weill (1970) and the

revised Kudo and Weill (Mathez, 1973) plagioclase-glass geothermometers.

The plagioclase-glass geothermometer is based on the distribution of

aluminum, silica, and alkalis between plagioclase and glass according

to the following reaction:

$$(NaSiO_{2.5})AlSi_2O_{5.5} + (Ca\ AlO_{2.5})AlSi_2O_{5.5} =$$
$$\text{plagioclase} \qquad\qquad \text{glass}$$

$$(Na\ SiO_{2.5})AlSi_2O_{5.5} + (Ca\ AlO_{2.5})AlSi_2O_{5.5} \qquad\qquad (4)$$
$$\text{liquid} \qquad\qquad \text{plagioclase}$$
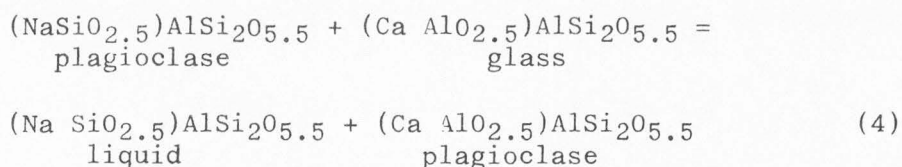
Temperatures obtained from the Kudo and Weill and the revised Kudo and

Weill geothermometers were $1241^{\circ}C$ and $1185^{\circ}C$ respectively (Table 10).

These temperatures appear to be generally higher than the temperatures

obtained using groundmass Fe-Ti oxides and olivine-clinopyroxene.

Tilley and Thompson (1970), in an investigation of melting and crystal-

lization relations of basalts of the Snake River Plain, found the

liquidus temperatures of the basalts to range from $1152^{\circ}C$ to $1207^{\circ}C$.

It appears that the plagioclase-glass temperature may be more consistent

with the liquidus temperature of the basalt rather than being represent-

ative of the temperature of groundmass crystallization.

The temperatures of crystallization determined for basalts of the
Gem Valley area are all within the range of crystallization temperatures
reported for basalts from the Snake River Plain (Stout and Nicholls,
1977).

Origin

Three processes of origin were examined for basalts from the Gem
Valley area: (1) low pressure (near-surface) fractional crystallization
of a parental magma; (2) accumulation of plagioclase to derive the
Group 2 lavas; and (3) partial melting of theoretical mantle compositions.

Fractional Crystallization

The AFM diagram (Figure 19) suggests that basalts of the Gem Valley
area follow a trend from an original MgO-rich magma toward increasing
iron content and finally toward increasing alkali content. This trend
is similar to that illustrated by basalts of the Snake River Plain and
Craters of the Moon (Stout and Nicholls, 1977; Leeman and Vitaliano,
1976). These trends are suggestive of a liquid line of descent whereby
the original MgO-rich liquid evolves toward an iron-rich liquid. Once
the point of Fe-Ti oxide precipitation is reached the liquid evolves in
a direction of increasing alkali content. In order to illustrate a
liquid line of descent controlled by fractional crystallization, it is
necessary to subtract the phenocryst compositions from possible parental
magmas to generate possible daughter magmas. This was tested using a
computer program which evaluates the best fit by a least squares solu-
tion for various parent-daughter combinations (e.g. Lowder and Car-
michael, 1970; Stormer, 1972).

The fractionation of Group 1 lavas to generate Group 2 lavas was tested using each Group 1 lava as a possible parent and subtracting its phenocryst phases to derive each Group 2 lava as a daughter product. The sum of squares of residuals for this series of fractionation models ranges from .6705 (GV76-4=parent, GV77-10=daughter) to 47.6503 (GV77-13=parent, GV77-14=daughter). Setting an acceptable limit to the sum of squares of residuals is arbitrary and a limit of 1.0 was set for this study. Only one parent-daughter combination has a sum of squares of residuals that is less than 1.0 (GV76-4, GV77-10; .6705). However, in order to derive GV77-10 from GV76-4, substantial amounts of plagioclase must be added to the Group 1 magma. This would appear to render unlikely the derivation of the Group 2 lavas from the Group 1 lavas only by means of fractional crystallization, but suggests that accumulation of plagioclase is significant.

Accumulation of Plagioclase

The hypothesis that the Group 2 lavas are derived by the accumulation of plagioclase in a magma of Group 1 composition was tested using the same least squares refinement technique just cited. The abundant plagioclase phenocrysts in the Group 2 lavas are suggestive of such an origin by accumulation. Group 1 lavas are used as possible parents and the plagioclase compositions of the Group 2 phenocrysts are used as the accumulated phase. Again only one parent-daughter combination has a sum of squares of residuals less than 1.0. Using GV76-6 as a parent, GV77-10 can be derived as a daughter product by adding 29 units of plagioclase phenocrysts for every 100 units of parent. This is consistent with the 30% plagioclase phenocrysts observed in GV77-10. A constraint placed on this hypothesis is that the density of the liquid must

be greater than the density of the crystallizing plagioclase to enable
the separation to take place. If the separating crystals had the same
composition as the observed phenocrysts of Group 2 basalts (labradorite)
they would have a density of approximately 2.7 g/cc. The density of the
liquid then must be greater than 2.7 g/cc. Stout (1975) reported a
density of 2.77 g/cc for basalts of the Craters of the Moon. These lavas
are more iron rich than the basalts of the Gem Valley area, and there-
fore the density of the Gem Valley lavas would be slightly less than
2.77 g/cc, suggesting that floatation of plagioclase is a viable mech-
anism. It is not possible to evaluate such parameters as magma viscosity,
conduit geometry, or the occurrence of flowage differentiation which
should be considered before fully accepting this hypothesis.

Partial Melting of the Mantle

To evaluate the hypothesis that the Gem Valley lavas were derived
as a result of partial melting of the mantle it is necessary to calcu-
late the percentage of partial melting from hypothetical mantle material.
This can be achieved by using the standard addition-subtraction diagram
technique from which percentages of partial melting can be calculated
(Bowen, 1928). Two model mantle compositions were used in this study:
(1) pyrolite (Green and Ringwood, 1967, p. 160, Table 20); and (2)
spinel-lherzolite (Bacon and Carmichael, 1973, p. 2, Table 1, #35).

When using a mantle composition of spinel-lherzolite, the percent-
age of partial melting ranges from .58% (GV78-1, GV77-10) to .99% (GV76-6).
The pyrolite mantle composition yields values for the percent of partial
melting which range from 5.02% (GV77-7) to 10.34% (GV76-6).

To determine the significance of these percentages, partial melting

of the upper mantle must be examined. Anderson and Sammis (1970) have shown that the presence of only trace amounts of water in the upper mantle will lower the melting temperature so that up to 1% of partial melting may occur without the production of magma. Furthermore, they also indicated that approximately 5% of partial melting is required before the migration of the molten phase occurs. Drury (1978) has determined that there is up to 9% partial melting in the upper mantle under the oceanic crust whereas under the continental crust the total partial melting is much lower although isolated pockets of partial melting may occur.

This suggests that the small percentages of partial melting of spinel-lherzolite (.58%-.99%) are not sufficient to produce the basalts found in Gem Valley. Although there is no quantitative estimate of partial melting beneath the continental crust it appears that the larger percentage of partial melting of pyrolite make it a more likely mantle composition. Again it is not possible to evaluate parameters such as magma viscosity, conduit geometry, or possible concentrations of fluid phases in the upper mantle in the vicinity of Gem Valley. These factors should be examined before fully accepting the pyrolite model.

SUMMARY

Comparison and Classification of Basalts of the Gem Valley Area

Chemical analyses of basalts of the Gem Valley area show that they
are low in silica, high in iron, and closely comparable to the basalts of
the Snake River Plain. However, the Group 1 Gem Valley lavas differ from
those of the Snake River Plain in the generally higher amounts of Al_2O_3
and lower amounts of MgO.

Based on normative constituents, basalts of the Gem Valley area
would be called olivine tholeiites. However, based on modal mineralogy,
Coombs' ratio, and the alkali-silica variation diagram, basalts of the
Gem Valley area would be classified as alkali-olivine basalts. This ap-
parent conflict in classification may be resolved by classifying basalts
of the Gem Valley area as transitional between the alkali-olivine basalts
and the olivine tholeiites. Care must be taken in using the transitional
classification. It must be remembered that there is no evidence in the
Gem Valley basalts to suggest that they have been derived either from
tholeiitic or alkali-olivine basalts. The transitional classification
is used only to indicate that the Gem Valley basalts have some character-
istics common to both tholeiitic basalt and alkali-olivine basalt.

Group 1 and Group 2 basalts of the Gem Valley area differ both
chemically and petrographically. The Group 1 basalts are more similar
to basalts of the Snake River Plain than are the Group 2 basalts. The
Group 2 basalts are more differentiated than the Group 1 basalts, having
generally lower MgO and higher TiO_2, Al_2O_3, Na_2O, K_2O, and P_2O_5.

Origin

Within the limits of this study, it has been found that the evolution
of the basalts of the Gem Valley area possibly occurred in two steps.
First, the Group 1 lavas may have formed as a result of partial melting
of a pyrolite mantle. Secondly, it is possible for the Group 2 lavas to
have formed as a result of the accumulation of plagioclase in a fraction-
ating magma of Group 1 composition. Investigation into the trace element
composition of these lavas would aid in the further evaluation of this
model.

REFERENCES

Albee, A.L. and Ray, L., 1970, Correction factors for electron probe microanalysis of silicates, carbonates, phosphates, and sulphates: Anal. Chem., v. 42, p. 1408-1414.

Anderson, D.L. and Sammis, C., 1970, Partial melting in the upper mantle: Phys. Earth and Planet. Inter., v. 17, p. 16-20.

Armstrong, F.C., 1953, Generalized composite stratigraphic section for the Soda Springs quadrangle and adjacent areas in southeastern Idaho: Intermountain Assoc. Petroleum Geologists 4th Ann. Field Conf., 1953: chart in pocket.

_____ 1969, Geologic map of Soda Springs quadrangle, southeastern Idaho: U.S. Geol. Survey Misc. Geol. Inv. Map I-557.

Armstrong, R.L., Leeman, W.P., and Malde, H.E., 1975, K-Ar dating, Quaternary and Neogene volcanic rocks of the Snake River Plain, Idaho: Amer. Jour. Sci., v. 275, p. 225-251.

Bacon, C.R. and Carmichael, I.S.E., 1973, Stages in the P-T path of ascending basalt magma; an example from San Quentin, Baja California: Contr. Mineral. and Petrol., v. 41, p. 1-22.

Bence, A.E. and Albee, A.L., 1968, Empirical correction factors for the electron microanalysis of silicates and oxides: Jour. Geol., v. 76, p. 382-403.

Bowen, N.L., 1928, The Evolution of the Igneous Rocks: Princeton University Press, 332p.

Bright, R.C., 1963, Pleistocene lakes Thatcher and Bonneville, southeastern Idaho: Univ. of Minnesota unpub. Ph. D. dissertation, 292p.

_____ 1967, Late Pleistocene stratigraphy in Thatcher basin, southeastern Idaho: Tebiwa, v. 10, no. 1, p. 1-7.

Brown, G.M. and Vincent, E.A., 1963, Pyroxenes from late stages of fractionation of the Skaergaard intrusion, East Greenland: Jour. Petrol., v. 4, p. 175-197.

Buddington, A.F. and Lindsley, D.H., 1964, Iron-titanium oxide minerals and synthetic equivalents: Jour. Petrol., v. 5, p. 310-357.

Carmichael, I.S.E., 1964, The petrology of Thingmuli, a Tertiary volcano in eastern Iceland: Jour. Petrol., v. 5, p. 435-460.

_____ 1967a, The iron-titanium oxides of salic volcanic rocks and their associated ferromagnesium silicates: Contr. Mineral. and Petrol., v. 14, p. 36-64.

_____ 1967b, The mineralogy of Thingmuli, a Tertiary volcano in eastern Iceland: Amer. Min., v. 52, p. 1815-1841.

_____ Hampel, J., and Jack, A.L., 1968, Analytical data on the U.S.G.S. standard rocks: Chemical Geol., v. 55, p. 246-263.

_____ Turner, F.J., and Verhoogen, J., 1974, Igneous Petrology: McGraw-Hill, N.Y., 739p.

Coombs, D.S., 1963, Trends and affinities of basaltic magmas and pyroxenes as illustrated on the diopside-olivine-silica diagram: Min. Soc. Amer. Sp. Paper No. 1, p. 227-250.

Elsdon, R., 1971, Clinopyroxenes from the Upper Layered Series, Kap Edvard Holm, East Greenland: Min. Mag., v. 38, p. 49-57.

Fenneman, N.M. and Johnson, D.W., 1946, Physical Divisions of the United States (map): U.S. Geol. Survey scale 1;7,000,000.

Green, D.H. and Ringwood, A.E., 1967, The genesis of basaltic magmas: Contr. Mineral. and Petrol., v.15, p. 103-190.

Kudo, A.M. and Weill, D.F., 1970, An igneous plagioclase geothermometer: Contr. Mineral. and Petrol., v. 25, p. 52-65.

Kuno, H., 1950, Petrology of Hokane volcano and adjacent areas, Japan: Bull. Geol. Soc. Amer., v. 61, p. 957-1020.

Kushiro, I., 1960, Si-Al relations in clinopyroxenes from igneous rocks: Amer Jour. Sci., v. 258, p. 548-554.

LeBas, M.J., 1962, The role of aluminum in igneous clinopyroxenes with relation to their parentage: Amer. Jour. Sci., v. 260, p. 267-288.

Leeman, W.P. and Rogers, J.J.W., 1970, Late-Cenozoic alkali-olivine basalts of the Basin-Range province, U.S.A.: Contr. Mineral. and Petrol., v. 25, p. 1-24.

_____ and Vitaliano, C.J., 1976, Petrology of the McKinney basalt, Snake River Plain, Idaho: Geol. Soc. Amer. Bull., v. 87, p. 1777-1792.

_____, _____, and Prinz, M., 1976, Evolved lavas from the Snake River Plain: Craters of the Moon National Monument, Idaho: Contr. Mineral. and Petrol., v. 56, p. 35-60.

Lowder, G.G. and Carmichael, I.S.E., 1970, The volcanoes and caldera of Talesea, New Britain: geology and petrology: Geol. Soc. Amer. Bull., v. 81, p. 17-38.

Mabey, D.R., 1971, Geophysical data relating to a possible Pleistocene overflow of Lake Bonneville at Gem Valley, southeastern Idaho: U.S. Geol. Survey Prof. Paper 750-B, p. B122-B127.

_____ and Armstrong, F.C., 1962, Gravity and magnetic anomalies in Gem Valley, Caribou County, Idaho: U.S. Geol. Survey Prof. Paper 450-D, p. D73-D75.

_____ and Oriel, S.S., 1970, Gravity and magnetic anomalies in the Soda Springs region, southeastern Idaho: U.S. Geol. Survey Prof. Paper 646-E, p. E1-E15.

MacDonald, R. and Katsura, T., 1964, Chemical composition of Hawaiian lavas: Jour. Petrol., v. 5, p. 82-133.

Mansfield, G.R., 1927, Geography, geology and mineral resources of part of southeastern Idaho: U.S. Geol. Survey Prof. Paper 152, 453p.

_____ 1929, Geography, geology and mineral resources of part of the Portneuf Quadrangle, Idaho: U.S. Geol. Survey Bull. 803, 112p.

Mathez, E.A., 1973, Refinement of the Kudo-Weill plagioclase thermometer in the system $MgO-FeO-Fe_2O_3-SiO_2$: Jour. Amer. Ceram. Soc., v. 39, p. 121-140.

Mitchell, C.M., Knowles, F.F., and Petrafeso, F.A., 1965, Areomagnetic map of the Pocatello-Soda Springs region, southeastern Idaho: U.S. Geol. Survey Geophys. Inv. Map GP-521.

Moore, J.G., 1966, Rate of palagonitization of submarine basalt adjacent to Hawaii: U.S. Geol. Survey Prof. Paper 550-D, p. D163-D171.

_____ and Evans, B.W., 1967, The role of olivine in the crystallization of the prehistoric Makaopuhi tholeiitic lava lake, Hawaii: Contr. Mineral. and Petrol., v. 15, p. 202-223.

Muan, A. and Osborn, E.F., 1956, Phase equilibria at liquidus temperatures in the system $MgO-FeO-Fe_2O_3-SiO_2$: Amer. Ceram. Soc. Jour., v. 39. p. 121-140.

Nicholls, J., Fiesinger, D.W., and Ethier, V.G., 1977, Fortran IV programs for processing routine electron microprobe data: Computers and Geosci., v. 3, p. 49-83.

Oriel, S.S., 1968, Preliminary geologic map of the Bancroft quadrangle, Caribou and Bannock Counties, Idaho: U.S. Geol. Survey open-file map.

_____, Mabey, D.R., and Armstrong, F.C., 1965, Stratigraphic data bearing on the inferred pull-apart origin of Gem Valley, Idaho: U.S. Geol. Survey Prof. Paper 565-C, P. C1-C4.

Osborn, E.F., 1959, Role of P_{O_2} in the crystallization and differentiation of basaltic magma: Amer. Jour. Sci., v. 257, p. 609-647.

Powell, M. and Powell, R., 1974, An olivine-clinopyroxene geothermometer: Contr. Mineral. and Petrol., v. 48, p. 249-263.

Powell, R. and Powell, M., 1977, Geothermometry and oxygen barometry using coexisting iron-titanium oxides: a reappraisal: Mineral. Mag., v. 41, p. 257-263.

Powers, H.A., 1960, A distinctive chemical characteristic of Snake River basalts of Idaho: U.S. Geol. Survey Prof. Paper 400-B, p. B298.

Simkin, T. and Smith, J.V., 1970, Minor element distribution in olivine: Jour. Geol., v. 78, p. 49-83.

Smith, A.L. and Carmichael, I.S.E., 1968, Quaternary lavas from the southern Cascades, western U.S.A.: Contr. Mineral. and Petrol., v. 19, p. 212-238.

Stormer, J.C., 1972, Mineralogy and petrology of the Raton-Clayton volcanic field, northeastern New Mexico: Geol. Soc. Amer. Bull., v. 83, p. 3299-3322.

_____ 1973, Calcium zoning in olivine and its relationship to silica activity and pressure: Geochim. et Cosmochim. Acta, v. 37, p. 1815-1821.

Stout, M.Z., 1975, Petrology of Idaho volcanics: Univ. of Calgary unpub. MS thesis.

_____ and Nicholls, J., 1977, Mineralogy and petrology of Quaternary lavas from the Snake River Plain: Can. Jour. of Earth Sci., v. 14, p. 2140-2156.

Thornton, C.P. and Tuttle, O.F., 1960, Chemistry of igneous rocks: I: Differentiation index: Amer. Jour. Sci., v. 258, p. 664-684.

Tilley, C.E. and Thompson, R.N., 1970, Melting and crystallization relations of Snake River basalts of southern Idaho, U.S.A.: Earth and Planet. Sci. Letters, v. 8, p. 79-92.

Wager, L.R. and Brown, G.M., 1967, Layered Igneous Rocks: W.H. Freeman and Co., San Francisco, 588p.

Yoder, H.S. and Tilley, C.E., 1962, Origin of basaltic magmas: an experimental study of natural and synthetic rock systems: Jour. Petrol., v. 3, p. 342-352.

APPENDIX I

Standards used in microprobe analyses, University of Utah, Department of Geology & Geophysics

Elem.	olivine	plagioclase	pyroxene	Fe-Ti oxides	pyroxene xenocryst	xenocryst rim
Si			opx-2525	tib-alb hess-18	opx-2525	hess-18
Ti			cpx wa-9	TiO_2 50-50	cpx wa-3	cpx wa-9
Al			cpx wa-9	52 nl 11	cpx wa-9	cpx wa-9
Fe	ol r2202 ol ys24		cpx wa-3	50-50	hess-18	hess-18
Mg	opx 2525		cpx wa-3	53 im 8 cpx wa-9	opx wa-1	opx wa-1
Ca	opx 2525 ol r2202	cb. byt. anorthite	cpx wa-3	sphene glass	opx wa-1	opx 2525
Na		lab. 667303	opx-2525 cpx wa-9 hess-18		cpx wa-9	opx-2525
K		orth. or-1				
Mn			hess-18	hess-18	hess-18	hess-18
V				53 im 8		
Cr				53 im 8		
Zn				53 im 8		